RESEARCH REPORT 1405-2

DEVELOPMENT OF HIGH PERFORMANCE GROUTS FOR BONDED POST-TENSIONED STRUCTURES

A. J. Schokker, B. D. Koester, J. E. Breen, and M. E. Kreger

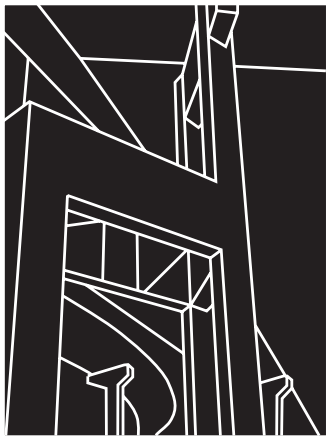

CENTER FOR TRANSPORTATION RESEARCH
BUREAU OF ENGINEERING RESEARCH
THE UNIVERSITY OF TEXAS AT AUSTIN

OCTOBER 1999

Technical Report Documentation Page

1. Report No.	2. Government Accession No.	3. Recipient's Catalog No.

4. Title and Subtitle	5. Report Date
DEVELOPMENT OF HIGH PERFORMANCE GROUTS FOR BONDED POST-TENSIONED STRUCTURES	**October 1999**
	6. Performing Organization Code
7. Author(s)	8. Performing Organization Report No.
A. J. Schokker, B. D. Koester, J. E. Breen, and Michael E. Kreger	Research Report 1405-2
9. Performing Organization Name and Address	10. Work Unit No. (TRAIS)
Center for Transportation Research The University of Texas at Austin 3208 Red River, Suite 200 Austin, TX 78705-2650	11. Contract or Grant No. Research Study 0-1405
12. Sponsoring Agency Name and Address	13. Type of Report and Period Covered
Texas Department of Transportation Research and Technology Transfer Office P.O. Box 5080 Austin, TX 78763-5080	Research Report (9/93-8/99)
	14. Sponsoring Agency Code

15. Supplementary Notes

Project conducted in cooperation with the U.S. Department of Transportation

16. Abstract

The use of post-tensioning in bridges can provide durability and structural benefits to the system while expediting the construction process. When post-tensioning is combined with precast elements, traffic interference can be greatly reduced through rapid construction. Post-tensioned concrete substructure elements such as bridge piers, hammerhead bents, and straddle bents have become more prevalent in recent years. Chloride-induced corrosion of steel in concrete is one of the most costly forms of corrosion each year. Coastal substructure elements are exposed to seawater by immersion or spray, and inland bridges may also be at risk due to the application of deicing salts. Corrosion protection of the post-tensioning system is vital to the integrity of the structure because loss of post-tensioning can result in catastrophic failure.

In bonded post-tensioned construction, the portland cement grout acts as a "last line of defense" for preventing chlorides from reaching the steel and initiating corrosion. Documentation for durability design of grout used in bonded post-tensioning is very limited. The purpose of the research is to develop a high performance grout for post-tensioning tendon injection. An optimum grout combines a high level of corrosion protection and desirable fresh properties such as fluidity and resistance to bleed. The recommended grouts were developed through a series of fresh property tests, accelerated corrosion tests, and a large-scale pumping test to simulate field conditions. Variables included water to cement ratio and numerous admixtures such as superplasticizer, anti-bleed chemicals, silica fume, fly ash, and corrosion inhibitors.

One high performance fly ash grout was developed for applications with small vertical rises, and a second high performance anti-bleed grout was developed for applications involving large vertical rises such as tall bridge piers.

17. Key Words	18. Distribution Statement
post-tensioned concrete, grout, fluidity, corrosion, admixtures, bleed, substructures, bridges	No restrictions. This document is available to the public through the National Technical Information Service, Springfield, Virginia 22161.

19. Security Classif. (of report)	20. Security Classif. (of this page)	21. No. of pages	22. Price
Unclassified	Unclassified	68	

Form DOT F 1700.7 (8-72) Reproduction of completed page authorized

DEVELOPMENT OF HIGH PERFORMANCE GROUTS FOR BONDED POST-TENSIONED STRUCTURES

by

A. J. Schokker, B. D. Koester, J. E. Breen, and M. E. Kreger

Research Report 1405-2

Research Project 0-1405
"DURABILITY DESIGN OF POST-TENSIONED
BRIDGE SUBSTRUCTURE ELEMENTS"

conducted for the
Texas Department of Transportation

In cooperation with the
U.S. Department of Transportation
Federal Highway Administration

by the
CENTER FOR TRANSPORTATION RESEARCH
BUREAU OF ENGINEERING RESEARCH
THE UNIVERSITY OF TEXAS AT AUSTIN

October 1999

IMPLEMENTATION

This report provides a detailed description of the experimental program for development of high performance grouts for bonded post-tensioned construction. A grout that can combine good corrosion protection with workability is a key component to the durability of a bonded post-tensioned system. Two grouts were developed through a series of fresh property tests, accelerated corrosion tests, and large-scale field tests. For horizontal applications (vertical rises up to 1 m), the recommended grout is a 0.35 water-cement ratio grout with 30% cement weight replacement fly ash and 4 ml/kg superplasticizer. For vertical applications (vertical rises up to 38 m), the recommended grout is a 0.33 water-cement ratio grout with 2% anti-bleed admixture.

Prepared in cooperation with the Texas Department of Transportation and the U.S. Department of Transportation, Federal Highway Administration.

DISCLAIMER

The contents of this report reflect the views of the authors, who are responsible for the facts and the accuracy of the data presented herein. The contents do not necessarily reflect the view of the Federal Highway Administration or the Texas Department of Transportation. This report does not constitute a standard, specification, or regulation.

NOT INTENDED FOR CONSTRUCTION,

PERMIT, OR BIDDING PURPOSES

J.E. Breen, P.E. #18479

M.E. Kreger, P.E. #65541

Research Supervisors

ACKNOWLEDGMENTS

We greatly appreciate the financial support from the Texas Department of Transportation that made this project possible. The support of the project director, Bryan Hodges (DES), and program coordinator, Richard Wilkison (DES), is also very much appreciated. We thank Project Monitoring Committee members, Gerald Lankes (CST), Ronnie VanPelt (BMT) and Tamer Ahmed (FHWA). We would also like to thank FHWA personnel, Jim Craig, Susan Lane and Bob Stanford, for their assistance on this project.

Initial grout research at the University of Texas by Trey Hamilton was very helpful to the further development of the Accelerated Corrosion Testing phase of the project.

Jeff West's continuous help and support were extremely valuable to the grout development portion of project 0-1405.

Research performed in cooperation with the Texas Department of Transportation and the U.S. Department of Transportation, Federal Highway Administration.

TABLE OF CONTENTS

LIST OF FIGURES

LIST OF TABLES

SUMMARY

The use of post-tensioning in bridges can provide durability and structural benefits to the system while expediting the construction process. When post-tensioning is combined with precast elements, traffic interference can be greatly reduced through rapid construction. Post-tensioned concrete substructure elements such as bridge piers, hammerhead bents, and straddle bents have become more prevalent in recent years. Chloride-induced corrosion of steel in concrete is one of the most costly forms of corrosion each year. Coastal substructure elements are exposed to seawater by immersion or spray, and inland bridges may also be at risk due to the application of deicing salts. Corrosion protection of the post-tensioning system is vital to the integrity of the structure because loss of post-tensioning can result in catastrophic failure.

In bonded post-tensioned construction, the portland cement grout acts as a "last line of defense" for preventing chlorides from reaching the steel and initiating corrosion. Documentation for durability design of grout used in bonded post-tensioning is very limited. The purpose of the research is to develop a high performance grout for post-tensioning tendon injection. An optimum grout combines a high level of corrosion protection and desirable fresh properties such as fluidity and resistance to bleed. The recommended grouts were developed through a series of fresh property tests, accelerated corrosion tests, and a large-scale pumping test to simulate field conditions. Variables included water to cement ratio and numerous admixtures such as superplasticizer, anti-bleed chemicals, silica fume, fly ash, and corrosion inhibitors.

One high performance fly ash grout was developed for applications with small vertical rises, and a second high performance anti-bleed grout was developed for applications involving large vertical rises such as tall bridge piers.

CHAPTER 1

INTRODUCTION AND BACKGROUND

Portland cement grout is often used in post-tensioned structures to provide bond between the tendon and the surrounding concrete and also as corrosion protection for the tendons. Grout for bonded post-tensioning is a combination of portland cement and water, along with any admixtures necessary to obtain required properties such as fluidity, thixotropy, and reduced permeability. The grout plays a crucial role in the corrosion protection of the system since it may be the "last line of defense" against chloride attack of the post-tensioning strands. An optimum grout combines desirable fresh properties along with good corrosion protection.

This report discusses the numerous grout designs that were evaluated through three phases of testing: fresh property tests, an accelerated corrosion test, and a large-scale clear duct test that simulated field conditions. The objective was to develop a grout with suitable workability and bleed resistance that also provided good corrosion protection. The key to development of an optimum grout is to lower permeability while minimizing the use of chemical admixtures that might have a detrimental effect on corrosion performance.

The research presented in this report describes the high performance grout development phase of a large project on durability of post-tensioned bridge substructure funded by the Texas Department of Transportation. Details about this project are found in Schokker.[25]

1.1 BACKGROUND

In bonded post-tensioned structures, the portland cement grout is often the last barrier against ingress of chlorides to the prestressing strand. Grouts with properties such as fluidity, low permeability, and bleed resistance can provide maximum protection when combined with proper grouting procedures.

1.1.1 Voids and Bleed

Voids can be formed in the post-tensioning duct from incomplete grouting, trapped air pockets, or from the evaporation of bleed water pockets. Top quality grout is of little benefit if poor grouting procedures result in large void formations, which provide no protection to the strand and no transfer of bond. Proper venting of the post-tensioning duct is critical for complete grouting. The void between the tendon and the post-tensioning duct is a very complex space. For instance, a parabolic shaped duct with a tensioned tendon may have a number of small voids of varying shapes and sizes, and a very stiff grout may not fill the interstices.[11] A more detailed discussion of venting and grout flow is included in Chapter 4.

Bleed lenses can form as a result of the separation of water from the cement. This sedimentation process is accentuated by the addition of seven-wire strand, which acts as a "water-transport mechanism."[27] The spaces within the individual twisted wires that form the strand are large enough to allow easy passage of water but not cement. Ducts with vertical rises will typically cause more bleed due to the increased pressure within the grout column. Intermediate bleed water lenses may form in tall vertical ducts, leaving a void through the cross-section of the duct exposing the tendon. Even in parabolic draped ducts, any bleed water will tend to gather near the highest intermediate points, leaving voids in the duct.

Grouts containing anti-bleed admixture, or thixotropic grouts, can be bleed resistant even when used in ducts with large vertical rises.[26] These grouts are able to retain their water even under high pressures and can eliminate significant void formation when proper grouting procedures are followed.

1.1.2 Silica Fume

Silica fume is a by-product from the manufacturing of silicon. Particles are spherical in shape with a mean diameter approximately 100 times finer than cement. Research has shown[1, 8, 10, 12, 14, 18, 24] that the addition of silica fume can increase compressive strength, reduce bleed and reduce permeability. The addition of silica fume results in an increased water demand. Thus, to maintain workability, a superplasticizer must be added to the grout. The dosage of superplasticizer increases with the amount of silica fume added, and the dosage may exceed limits recommended by the superplasticizer manufacturer.[24] Research with varying amounts of silica

fume addition has shown that silica fume addition is optimized at around 5-7% cement weight replacement.[24, 34] Silica fume grouts have also been found to be thixotropic in nature; that is, they remain sticky and cohesive at rest, but retain their fluidity when agitated.[1, 12]

Silica fume grouts tend to have a lower pH than plain grouts, and therefore the concentration of chlorides necessary to breakdown the passive layer on the steel may be reduced. However, this effect is considered small in comparison to the reduced chloride diffusivity rates found in silica fume grouts.[14]

1.1.3 Fly Ash

Although silica fume has been used widely in some parts of the country, the use of fly ash as a pozzolan is much more common in Texas. Fly ash particles are spherical in shape and are the by-product of the combustion of coal. Two classes of fly ash are commonly used in concrete. Class F fly ashes typically have low amounts of calcium and Class C ashes typically have higher calcium contents. Fly ash tends to reduce bleed and reduce permeability, although silica fume has a greater effect on these properties. Compressive strength can be increased, but strength gain tends to be slower for fly ash grouts. Water requirements are also reduced due to the dispersion and deflocculation of the cement particles from the fly ash.[31] The addition of fly ash reduces the dosage of superplasticizer needed to maintain adequate fluidity in grouts.

1.1.4 Corrosion Inhibitors

Many types of corrosion inhibitors are on the market today. They are intended to slow the corrosion process of steel in concrete without adversely affecting other properties and are typically included as an admixture in the fresh concrete. Corrosion inhibitors can be divided into three basic types by the method in which they slow the corrosion process.[21, 28]

Anodic Inhibitors (Passive System)

Anodic inhibitors react with the steel to form a protective film, and proper dosage depends on the amount of chlorides penetrating the concrete. If the amount of chlorides is too high for the dosage of corrosion inhibitor, then all of the anodic sites are not eliminated and corrosion continues at a rate greater or equal to that of untreated concrete. The popular corrosion inhibitor, Calcium Nitrite, is an anodic inhibitor.

Cathodic Inhibitors (Active System)

Cathodic inhibitors form a barrier around the cathodic site to reduce chloride ingress. These inhibitors tend to be less efficient than anodic inhibitors. Silica fume is an example of a cathodic inhibitor.

Mixed Inhibitors (Passive-Active System)

Mixed inhibitors combine the inhibiting traits of both the anodic and cathodic type inhibitors.

Calcium Nitrite is one of the most common corrosion inhibitors used in the United States. Numerous studies have shown that Calcium Nitrite slows corrosion when added to concrete,[6, 7, 16] and it has been used successfully in the United States since the 1970s. Limited research is available on the use of Calcium Nitrite in cement grouts. Some research has shown a reduction in time to corrosion for grouts with Calcium Nitrite.[15, 17] This problem is discussed in detail in Chapter 3. Many new corrosion inhibitors are being introduced, including amino-alcohol-based inhibitors[19, 21] that may avoid some of the problems associated with Calcium Nitrite.

1.1.5 Condition of Post-Tensioned Bridges Today

Corrosion of post-tensioned bridges does not appear to be a major problem at this point,[22, 28] although many post-tensioned structures are relatively new. One of the problems with internal post-tensioning is that inspection of the tendons and anchorage is difficult. Often problems are found by accident during other work on the bridge or during demolition of redundant structures.[35] By far the most common problem found in corroded post-tensioning tendons is poorly grouted or completely ungrouted tendons. After three publicized collapses of post-tensioned structures, the United Kingdom placed a moratorium on the use of grouted post-tensioned structures in 1992. The three confirmed collapses all involved internally post-tensioned structures and the collapses occurred without warning. These collapses were the Bickton Meadows bridge and Ynys-y-Gwas bridge in the United Kingdom and a bridge over the River Schelde in Belgium. In 1996, the United

Kingdom's Working Party completed a document entitled *Durable Bonded Post-Tensioned Bridges*[35] and the moratorium on bonded post-tensioning in the UK was lifted based on adoption of these recommendations. Due to the importance of proper grouting, the document includes detailed grouting specifications, and information for training grouting technicians.

1.2 OBJECTIVES

The objectives of the overall research program 0-1405 are as follows:

- To investigate the effect of post-tensioning on durability
- To investigate the relative corrosion performance of a number of variables related to post-tensioned structures
- To develop a high-performance grout for corrosion protection in bonded post-tensioned construction
- To develop recommendations and guidelines for durable bonded post-tensioned bridge substructures

The research presented in this report covers only the development of a high-performance grout for bonded post-tensioning through a series of fresh property tests, accelerated corrosion tests, and large-scale field trials.

1.3 PROJECT SCOPE

The research presented in this report represents part of a large project funded by the Texas Department of Transportation, entitled, "Durability Design of Post-Tensioned Bridge Substructures" (Project 0-1405). Nine reports are scheduled to be developed from this project as listed in Table 1.1.

Table 1.1: Proposed Project 0-1405 Reports

Number	Title	Estimated Completion
1405-1	State of the Art Durability of Post-Tensioned Bridge Substructures	1999
1405-2	Development of High Performance Grouts for Bonded Post-Tensioned Structures	1999
1405-3	Long Term Post-Tensioned Beam and Column Exposure Test Specimens: Experimental Program	1999
1405-4	Corrosion Protection for Bonded Internal Tendons in Precast Segmental Construction	1999
1405-5	Interim Conclusions, Recommendations and Design Guidelines for Durability of Post-Tensioned Bridge Substructures	1999
1405-6	Final Evaluation of Corrosion Protection for Bonded Internal Tendons in Precast Segmental Construction	2002
1405-7	Design Guidelines for Corrosion Protection for Bonded Internal Tendons in Precast Segmental Construction	2002
1405-8	Long Term Post-Tensioned Beam and Column Exposure Test Specimens: Final Evaluation	2003
1405-9	Conclusions, Recommendations and Design Guidelines for Durability of Post-Tensioned Bridge Substructures	2003

Several dissertations and theses at The University of Texas at Austin were developed from the research from Project 0-1405. These documents may be valuable supplements to specific areas in the research and are listed in Table 1.2 for reference.

Table 1.2: Project 0-1405 Theses and Dissertations, The University of Texas at Austin

Title	**Author**	**Date**
Masters Theses		
"Evaluation of Cement Grouts for Strand Protection Using Accelerated Corrosion Tests"	Bradley D. Koester	12/95
"Test Method for Evaluating Corrosion Mechanisms in Standard Bridge Columns"	Carl J. Larosche	8/99
"Test Method for Evaluating the Corrosion Protection of Internal Tendons Across Segmental Bridge Joints"	Rene P. Vignos	5/94
Ph.D. Dissertations		
"Improving Corrosion Resistance of Post-Tensioned Substructures Emphasizing High Performance Grouts"	Andrea J. Schokker	5/99
"Durability Design of Post-Tensioned Bridge Substructures"	Jeffrey S. West	5/99

CHAPTER 2

FRESH PROPERTY TESTING

The first phase of grout testing was the fresh property test phase. Only grouts possessing adequate fresh properties were subsequently considered for the accelerated corrosion test phase. This performance based fresh property testing was beneficial for selecting the appropriate dosages of admixtures and pozzolans. An optimum grout is fluid enough to be workable while providing good corrosion protection to the prestressing strands. Bleed resistance is also an important consideration, especially in situations where there will be changes in duct elevation. Set time and strength are also fresh properties that should be considered.

Pozzolans such as fly ash and silica fume may be beneficial to corrosion protection by reducing grout permeability, but their effects on fresh properties should also be investigated. Often the admixtures used to attain certain desirable properties may adversely effect other properties. When several admixtures are used simultaneously it is also necessary to test their behavior as a group to insure compatibility and to achieve optimum combinations.

During all phases of grout testing, the Texas Department of Transportation (TxDOT) standard grout was included as a comparison. This grout has a 0.44 water-cement ratio with 1% cement weight of Intraplast-N expansive admixture.

2.1 MIX DESIGN

Grouts tested contained ASTM Type I cement and various admixtures. Grouts used for the fresh property testing and large scale duct testing contained potable water while grouts for the accelerated corrosion testing contained distilled water as a precaution against introducing error in testing. A drill with a paddle mixer attachment was used to mix the grout.

Unless otherwise noted, cwt refers to cementitious (cement and pozzolans) weight and percentages given of pozzolans are replacement percentages of cement by weight. Water-cementious (cement and pozzolans) ratios are given as w/c.

2.1.1 Admixtures

Many types of admixtures were tested to evaluate their effect on the fresh properties and corrosion protection properties of the grout. Products from several different manufacturers were included, and a list of the products chosen is shown in Table 2.1.

Table 2.1: List of Admixtures Chosen

Admixture Type	*Brand Name*	*Manufacturer*
Superplasticizer	Rheobuild 1000	Master Builders
Expansive	Intraplast-N	Sika Corporation
Anti-bleed	Sikament 300SC	Sika Corporation
Corrosion Inhibitor (Calcium Nitrite)	DCI	W.R. Grace
Fly Ash	Class C	
Silica Fume	Sikacrete 950DP	Sika Corporation

2.2 FLUIDITY

Fluidity testing indicates the workability of the grout. Two variations of ASTM C939, *Standard Test Method for Flow of Grout for Pre Placed-Aggregate Concrete*[4] were used. For non-thixotropic grouts (grouts without anti-bleed admixture), the cone was filled to the indicated level and the time for the grout to empty the cone was recorded. For thixotropic grouts, the cone was filled to the top and the time for 1 liter of grout to empty from the cone was recorded. If the grout flow stopped prior to the end of the test, the test was judged a failure. At the time of testing, the Post-Tensioning Institute (PTI) was working on the *Guide Specification for Grouting of Post-Tensioned Structures.*[23] The draft available at the time suggested a flow cone time to exit between 20-30 seconds. Therefore, grouts passing this requirement in fluidity testing were considered to have "passed". The flow cone time to exit of identical mixes may vary considerably depending on the ambient temperature. Since all of the fluidity testing was performed in the Texas summer heat, this was taken into consideration in choosing grouts for the accelerated corrosion testing. After completion of the testing in this program, the Working Party of the Concrete Society[35] released an extensive technical report to remove the restriction on grouted post-tensioned bridges in the United Kingdom. This report recommends a flow cone time to exit of 25 seconds or less.

The trial grout designs evaluated are shown in Table 2.2 along with the corresponding fluidity test results. Most grouts tested had a maximum water-cement ratio of 0.35, and admixtures and pozzolans were adjusted to achieve the desired properties. The 0.35 water-cement ratio was chosen for two main reasons: extensive fluidity testing had already been performed on grouts with water-cement ratios around 0.40 by Hamilton[15] at the University of Texas at Austin for his Ph.D. dissertation on corrosion protection systems for bridge cable stays, and the trend in grouting seems to be leaning toward very low water-cement ratio grouts that have proven effective in providing corrosion resistance.[23, 35]

Grouts indicated with an asterisk in Table 2.2 were considered promising and were further evaluated in subsequent corrosion tests. Mix design #2 in Table 2.2 was included in further corrosion testing as a base case plain grout.

2.3 STANDARD BLEED RESISTANCE

Bleed can be much more of a concern in nonvertical grouted ducts than it is in the average concrete member. Bleed water that is forced out of the grout cannot simply evaporate from the top surface as it does in concrete members, but remains trapped in the post-tensioning duct. The trapped bleed water tends to migrate to the highest elevation in the duct where it collects and forms a bleed lense. The bleed water eventually evaporates and often a void is left in its place. The void can be particularly detrimental to the system if it exposes the post-tensioning tendon to corrosive substances that may penetrate the concrete cover and duct.

A standard bleed test indicates the bleed properties of a grout under atmospheric conditions. A modified version of ASTM C940, *Standard Test Method for Expansion and Bleeding of Freshly Mixed Grouts for Preplaced-Aggregate Concrete in the Laboratory*[3] was used. A 1000 ml graduated cylinder was filled with 800 ml of fresh grout and the volume of bleed water was measured over time. A modification was made to include a three-strand bundle in the grout column to simulate the wicking effects of a post-tensioning tendon. The PTI draft specification[23] limits maximum bleed to 1% of grout volume. Many grouts with poor fluid properties were not included in the bleed testing. Results from this test are included in Table 2.3. The mixes correspond to those given in Table 2.2. The majority of the grouts were under the PTI maximum bleed volume of 1%, suggesting that the test is not very sensitive. Since the test is run under standard atmospheric conditions in a cylinder with a grout height of approximately ½ meter, the bleed resistance tested is only applicable for ducts with vertical rises less than this height.

Table 2.2: Mix Designs and Fluidity Results

Mix #	*w/c*	*Admixtures*	*Fluidity (sec)*
1	0.35	none	null
***2**	0.40	none	195
3	0.35	4 ml/kg cwt Rheobuild	null
4	0.35	6 ml/kg cwt Rheobuild	38
5	0.35	8 ml/kg cwt Rheobuild	27
6	0.35	15% cwt Fly Ash, 4 ml/kg cwt Rheobuild	31
7	0.35	25% cwt Fly Ash, 2 ml/kg cwt Rheobuild	73
***8**	0.35	30% cwt Fly Ash, 4 ml/kg cwt Rheobuild	29
9	0.30	30% cwt Fly Ash, 80 ml/kg cwt Rheobuild	42
10	0.35	15% cwt Sikacrete, 6 ml/kg cwt Rheobuild	null
11	0.35	15% cwt Sikacrete, 8 ml/kg cwt Rheobuild	94
12	0.35	15% cwt Sikacrete, 12 ml/kg cwt Rheobuild	66
13	0.35	15% cwt Sikacrete, 14 ml/kg cwt Rheobuild	61
***14**	0.35	15% cwt Sikacrete, 16 ml/kg cwt Rheobuild	34
15	0.35	25% cwt Sikacrete, 16 ml/kg cwt Rheobuild	null
16	0.35	25% cwt Sikacrete, 18 ml/kg cwt Rheobuild	130
17	0.40	1.7% cwt Sikament	12
18	0.35	1.9% cwt Sikament	15
***19**	0.33	2.0% cwt Sikament	30
20	0.30	2.6% cwt Sikament	65
21	0.35	25% cwt Fly Ash, 2.1% cwt Sikament	11
22	0.35	25% cwt Fly Ash, 1.7% cwt Sikament	13
23	0.35	30% cwt Fly Ash, 1.7% cwt Sikament	11
24	0.35	10% cwt Sikacrete, 2.2% cwt Sikament	170
25	0.35	5% cwt Sikacrete, 4.0% cwt Sikament	41
26	0.35	10% cwt Sikacrete, 2.8% cwt Sikament, 4 ml/kg cwt Rheobuild	40
27	0.35	15% cwt Sikacrete, 2.4% cwt Sikament, 12 ml/kg Rheobuild	95
28	0.35	5% cwt Sikacrete, 20% cwt Fly Ash, 2.2% cwt Sikament	30
29	0.35	10% cwt Sikacrete, 15% cwt Fly Ash, 2.2% cwt Sikament	134
30	0.35	10% cwt Sikacrete, 15% cwt Fly Ash, 2.2% cwt Sikament, 8 ml/kg cwt Rheobuild	43
***31**	0.44	TxDOT Standard Grout (0.9% Intraplast-N)	31

*grouts chosen for ACTM testing

2.4 PRESSURIZED BLEED RESISTANCE

A pressurized bleed test was developed by Schupack[26] to simulate conditions where grout ducts experience a change in elevation. The grout was tested using a funnel manufactured by Gelman Sciences. The grout was placed in the funnel and pressurized with air through a stem at the top. The bottom of the funnel contained a stainless steel screen that supported a glass fiber filter that filtered out bleed water from the grout. Ten minutes

after the funnel was filled with grout, the sample was pressurized in 69.0 kPa increments and held for 3 minutes at each increment up to 552 kPa where it was held for 30 minutes before pressure was released. Readings were taken at each increment, and pressure at first bleed and loss of pressure were recorded. At the time of testing, no established standard existed, so performance was based on tests by Hamilton[15] with a recommended maximum bleed of 2% of the grout sample volume at 345 kPa. The pressure applied in the Gelman test can be translated into height of vertical rise by Equation 2-1:[15]

$$p = hg\left(\gamma_g - \gamma_w\right) \tag{2-1}$$

where p is the pressure, h is the height of grout column, γ_g is the density of grout (1950 kg/m^3), and γ_w is the density of water (1000 k/m^3). Therefore, an applied pressure of 345 kPa should be approximately equivalent to the pressure at the base of a 38 m tall grout column.

The results for the Gelman pressure test are included in Table 2.3. The percentage volume of bleed water at 345 kPa is given in the column labeled "Pressure Bleed". Grouts that bled before any pressure was applied to the funnel were labeled as "instant" bleed. The column labeled "Gelman First Bleed" gives the applied pressure reading when bleed was first observed. The last column gives the highest pressure value obtained prior to loss of pressure in the funnel (which is indicated by air leakage from the bottom of the grout column and a drop in pressure). Those grouts that did not experience pressure loss throughout the test were labeled as "no loss". These grouts showed the strongest anti-bleed characteristics.

The only grouts that had less than 2% bleed at 345 kPa were grouts that contained anti-bleed admixture. This test is significantly more discriminating than the standard bleed test and is intended to test grouts used in applications involving large vertical rises. The PTI draft specification recommends the use of the Gelman test, but does not give suggested values of acceptable bleed. A large gap in pressurized bleed performance exists between grouts that include an anti-bleed admixture and grouts that do not. Grouts that had less than 2% bleed at 345 kPa should be adequate in vertical rises up to 38 m. The grouts that did not contain anti-bleed admixture typically began to bleed instantly in the Gelman filter so no estimate of safe vertical rise can be obtained. Field trials may be necessary for grouts without anti-bleed admixtures that are intended for use in ducts with small vertical rises (1-5 m). In bridge substructure applications, pressurized bleed tests for grouts may be very relevant in structural components with large vertical rises (5-38 m) such as tall piers, but not so important when elevation change is minimal as in straddle bents.

Table 2.3: Standard Bleed and Pressurized Bleed Results

Mix #	*Standard Bleed (%)*	*Pressure Bleed* (%)*	*Gelman First Bleed (kPa)*	*Gelman Pressure Loss (kPa)*
1	-	-	-	-
2	-	-	-	-
3	-	-	-	-
4	3.8	instant	0	276
5	3.8	instant	0	207
6	3.8	instant	0	138
7	1.2	instant	0	138
8	0.6	instant	0	276
9	0	3.5	69	no loss
10	-	-	-	-
11	0.6	<	69	276
12	0.6	instant	0	138
13	-	-	-	-
14	0.6	instant	0	138
15	-	-	-	-
16	0	3.3	69	414
17	1.3	2.5	138	no loss
18	0	2.6	138	no loss
19	0	1.9	138	no loss
20	-	-	-	-
21	0	6.3	69	552
22	0	6.8	69	no loss
23	0	5.9	138	552
24	0	instant	0	138
25	0	<	276	no loss
26	0	1.6	207	no loss
27	0	1.0	845	no loss
28	0	3.0	69	no loss
29	-	-	-	-
30	0	1.6	207	no loss
31	0.6	instant	0	138

*bleed at 345 kPa from Gelman pressure test
< indicates loss of pressure before 345 kPa
- indicates test not run
1 psi = 6.895 kPa

2.5 SET TIME

The PTI draft specifications[23] recommend that set time be determined from ASTM C953 *Standard Test Method for Time of Setting of Grouts for Preplaced Aggregate Concrete in the Laboratory*[5] and that the set time should be greater than 3 hours and less than 12 hours. Only selected grout designs were chosen to check set time. Since anti-bleed admixture is known to increase set time, the grout design with the largest dose of anti-bleed

(4% cement weight of anti-bleed admixture) was tested and had a set time of 10 hours. The largest dosage of anti-bleed admixture used in a grout that proceeded to the accelerated corrosion tests was 2% (cement weight).

2.6 STRENGTH

A minimum value of compressive strength is desirable. The PTI draft[23] specifies ASTM C942, *Compressive Strength of Grouts for Preplaced Aggregate Concrete in the Laboratory*,[2] to test grout cube strength. The PTI draft gives a minimum compressive strength of 21 MPa at 7 days and 35 MPa at 28 days. Cube specimens were tested for grout used in a large-scale beam exposure testing program funded by the Texas Department of Transportation.[25] Average 7 day and 28 day strengths for the three types of grout included in the large scale specimens are shown in Table 2.4. The fly ash grout and anti-bleed grout easily meet the strength requirements, while the TxDOT grout is lower than the 28 day requirement given by the latest PTI draft.[23] The draft that was available at the time of testing recommended a 28 day strength exceeding 27 MPa.

Table 2.4: Compressive Strength Comparison

Mix #	***w/c***	***Admixtures***	***Strength (MPa)***	
			7 day	***28 day***
8	0.35	30% cwt Fly Ash 4 ml/kg superplasticizer	39.2	43.5
19	0.33	2% anti-bleed admixture	53.7	55.4
31	0.44	0.9% cwt Intraplast-N (TxDOT grout)	24.5	28.4

2.7 CONCLUSIONS

Results from the fresh property tests indicate that for water-cement ratios in the tested range, a superplasticizer is necessary to maintain fluidity. The addition of fly ash increases fluidity while the addition of silica fume decreases fluidity.

Standard bleed is reduced with reduced water-cement ratio and is reduced in grouts containing fly ash or silica fume, while superplasticizer has an adverse effect on standard bleed. Grouts containing anti-bleed admixture experienced no significant bleed during the standard bleed test. The only grouts that passed the pressurized bleed test were those containing the anti-bleed admixture, thus an anti-bleed admixture should be added to grouts intended for use in structural members with large vertical rises (above 5 m).

CHAPTER 3

ACCELERATED CORROSION TESTING

Grouts that performed well in the fluidity test phase were advanced to the accelerated corrosion testing phase. Also tested in this phase were the TxDOT standard grout and a plain grout with 0.40 water-cement ratio that was used as a baseline to check the repeatability of the present tests with previous tests.

3.1 THE ACCELERATED CORROSION TESTING METHOD (ACTM)

An accelerated corrosion testing method was developed by Thompson, Lankard, and Sprinkel[32] in a FHWA sponsored study and was refined at The University of Texas at Austin by Hamilton[15] and further refined by Koester.[17] The corrosion test uses anodic polarization to accelerate corrosion by providing a potential gradient, driving negatively charged chloride ions through the grout to the steel. The test was intended to provide a fairly simple and quick method for the relative comparison of grout corrosion protection under extremely harsh corrosive conditions.

3.1.1 Specimen Preparation

The test specimen consists of a short length of prestressing strand in a grouted clear PVC mold casing as shown in Figure 3.1. A plastic spacer is fitted in the bottom of the PVC cap to keep the strand spaced concentrically within the PVC casing. The end cap is then glued to the PVC casing. The 12.7 mm diameter strand is beveled at one end for ease of insertion into the spacer, and the strand is cleaned with acetone to remove surface contamination. The grout mix is prepared using distilled water and is placed into the casing in three stages. Before the strand is inserted, the PVC casing is filled approximately 1/3 up its depth with grout. The strand is then inserted into the assembly. The casing is filled in two more equal lifts, and the strand is slowly rotated between lifts to allow air bubbles to escape. A spacer is inserted at the top of the casing to hold the strand in place. The specimens are placed in racks and allowed to cure for eight days in a humidity chamber.

After eight days of curing, a portion of the PVC casing is removed with a rotary wire brush, taking care not to damage the grout. Two radial cuts are made first, followed by two longitudinal cuts. After removal of the casing, the specimen is immediately wrapped in a wet towel to prevent cracking prior to immersion in the NaCl solution.

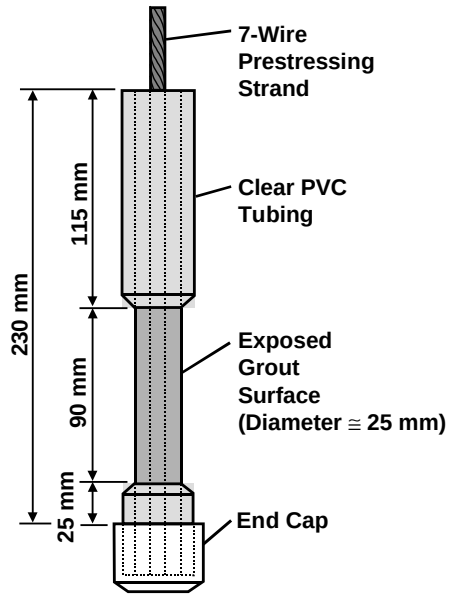

Figure 3.1: Specimen Dimensions

3.1.2 Instrumentation

During testing, the specimens are immersed in a 5% NaCl solution in a 3000 ml beaker. The beaker is covered with a Plexiglas cap with holes for the electrodes. A gel-filled saturated calomel electrode manufactured by Fisher Scientific is used as a reference electrode. Corrosion potential (E_{corr}) is measured from the reference electrode relative to the working electrode, and the corrosion current (i_{corr}) is found by measuring the voltage across a 100 Ω resistor in line with the lead on the counter electrode. A diagram of one of the 12 experimental stations is shown in Figure 3.2, and a picture of the entire test setup is shown in Figure 3.3.

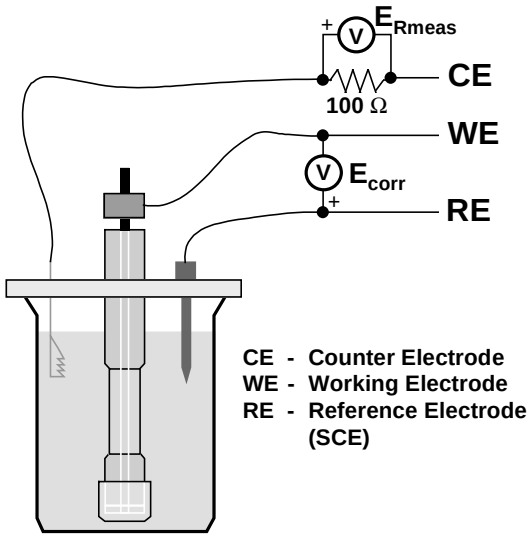

Figure 3.2: Schematic of ACTM Station

Figure 3.3: ACTM Test Setup

The 12 stations are connected to two, six-channel potentiostats (in this case a Cortest Model 125 is used for six stations and an Electrosynthesis Company Model 440 is used for the remaining six stations). The output leads from each potentiostat are connected to a Campbell Scientific AM416 Relay Multiplexer. The multiplexer sends data to a Campbell 21X Micrologger, one station at a time. The measured potential (E_{meas}) and the corrosion potential (E_{corr}) are recorded at 30 minute intervals during the test. I_{corr} can then be calculated from E_{meas}. Data from the Micrologger are downloaded daily to a PC.

Immediately after the section of casing has been removed from the specimens, they are connected to the electrodes and allowed to soak in the NaCl solution for approximately 15 minutes during which time the free corrosion potential is recorded by hand. Testing begins by applying a potential of +200 mV_{SCE} (approximately 400 mV above the free corrosion potential) to each station.

3.1.3 Anodic Polarization

Anodic polarization as used in the Accelerated Corrosion Test Method involves applying a potential to the specimen to speed the onset of corrosion. This applied potential (or voltage) is more positive than the free corrosion potential of the specimen, and the potential gradient developed tends to drive the negatively charged chloride ions through the grout to the steel surface. The applied potential can cause a shift in passivity for an active-passive metal. Hamilton developed potentiodynamic curves for several of his ACTM specimens as

shown in Figure 3.4. An applied potential of +200 mV_{SCE} would be in the passive range, while a higher potential such as +600 mV_{SCE} would be in the transpassive range.

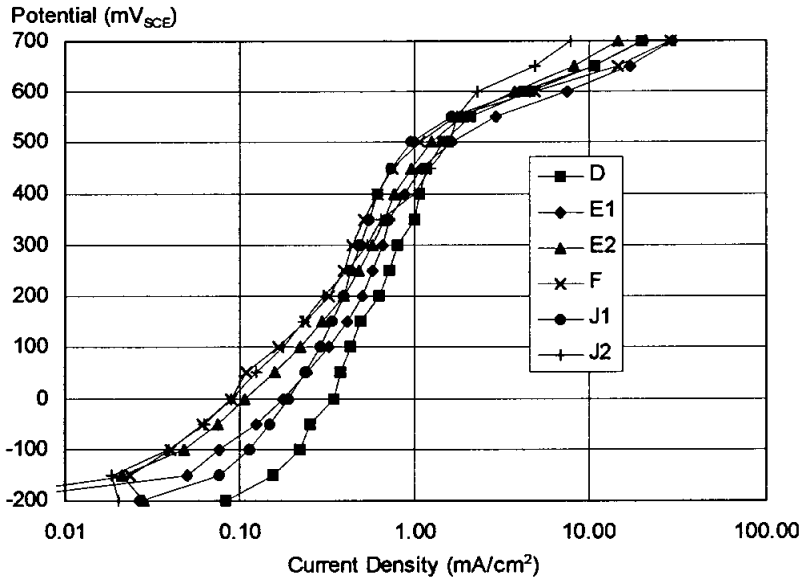

D, E1, E2 = antibleed admixture
F = antibleed and calcium nitrite
J1, J2 = antibleed and silica fume

Figure 3.4: Polarization Curves for Grouted Prestressing Steel Specimens[15]

3.1.4 Ohmic Electrolyte Resistance

A major problem with corrosion testing that utilizes anodic polarization (or any method that uses an applied current or potential), is the ohmic resistance or IR drop of the electrolyte. The IR refers to the applied current (I_{app}) times the effective ohmic resistance (R_Ω) between the reference and working electrodes. Poor conducting electrolytes (such as grout) can result in large IR drop errors. The IR drop can be minimized by moving the reference electrode close to the surface of the working electrode.[13] However, in testing grouted specimens, it is impracticable to make the applied potential measurement at the interface between the steel and the grout. The applied potential reading in the ACTM tests is made at the tip of the reference electrode and may cause actual applied potentials to differ depending on the ohmic resistance of the grout.

For the purposes of the ACTM (relative grout performance), the IR drop would not be a problem if the value was consistent for all types of grouts. Unfortunately, the IR drop of a grout changes with the addition of admixtures and pozzolans. Admixtures such as calcium nitrite have been found to reduce the ohmic resistance of concrete,[9] while silica fume and fly ash increase the ohmic resistance in concrete.[15]

It is possible that differences in IR drop bias the ACTM toward grouts with higher ohmic resistances since the actual applied potential would be lower than the applied potential for grouts with lower ohmic resistances. However, a high ohmic resistance is a desirable corrosion protection property since it tends to reduce the corrosion current, so the bias may be toward grouts with good corrosion protection. The extent of the effect of the IR drop is the more relevant issue. The potentiodynamic curves from Hamilton shown in Figure 3.4 do not show significant differences in ohmic resistance between grout types at +200 mV_{SCE} (the applied potential in the present study). In fact, one of the calcium nitrite grouts and one of the silica fume grouts have very similar ohmic resistances at this level. More in-depth studies of the effect of IR drop are necessary to satisfactorily determine the extent of this influence.

3.2 PREVIOUS ACTM STUDIES

3.2.1 The Original ACTM

Development of the original ACTM is discussed in the FHWA report FHWA-RD-91-092.[32] The original specimen consisted of a 267 mm long, 12.7 mm diameter seven-wire prestressing strand in a grouted 19 mm diameter pipe. Specimens were cured for 28 days and then a 114 mm section of the casing was removed. Tests consisted of uncracked and precracked specimens. The test procedure was similar to that discussed in the previous section, but the applied potential for the majority of the tests was +600 mV_{SCE}. The mix designs chosen for the FHWA study are shown in Table 3.1, and a summary of the results are shown in Table 3.2.

Table 3.1: Original ACTM Mix Designs[32]

Test	*w/c*	*Admixtures*
P1	0.44	None
P2	0.65	None
P3	0.32	33% cwt Fly Ash, 52% cwt Silica Sand, 0.05% cwt Polysaccharide Gum, 26 ml/kg cwt HRWR*
P4	0.365	11% cwt Silica Fume (addition), 10-36 ml/kg cwt HRWR*
P5	0.29	31.5% Latex Polymer Modifier, 10 ml/kg cwt HRWR*
P6	0.365	0.75% cwt Aluminum Powder, 0.01% cwt Polysaccharide Gum, 21 ml/kg HRWR*
P7	0.44	29 l/m^3 Calcium Nitrite (DCI – W.R. Grace)

*High-range water reducer

Table 3.2: Original ACTM Summary of Times to Corrosion[32]

Test	*Potential*	*Time to Corrosion (hours)*			
	mV_{SCE}	*Uncracked*	*Ave*	*Precracked*	*Ave*
P1a	600	140, 205, 170, 180	174	50, 150, 25, 130	89
P1b	0	290, 65	178	none	-
P2	0	50, 25, 27, 20	31	none	-
P3	600	335, 535, 350, 450	418	25, 0, 0	25
P4	600	245, 150, 650, 135	295	25, 0	25
P5	600	335, 125, 150, 200, 220, 390	237	90, 0, 0, 0	90
P6	0	190, 140, 200, 140	227	10, 2, 0, 20	8
P7a	600	70, 105, 160, 180	129	55, 40	48
P7b	0	546, 430, 875, 1000	713	none	-

The researchers felt that the poor performance of the grouts containing the corrosion inhibitor calcium nitrite may have been due to the high polarization potential of +600 mV_{SCE}. Calcium nitrite needs the passive layer on the steel to work and may actually accelerate corrosion when the layer is not present. The higher potential of +600 mV is likely to be in the transpassive region for the steel, so the researchers ran a limited number of tests at 0 mV_{SCE}. The results at the lower potential are more favorable for the calcium nitrite grouts, but only a limited number of specimens were run at the lower potential for comparison. The results for the other specimens showed an increase in corrosion protection with lowered water-cement ratio and with the addition of fly ash and silica fume.

3.2.2 ACTM Studies at The University of Texas at Austin

Initial ACTM tests at The University of Texas at Austin were carried out by Hamilton.[15] Hamilton modified the original ACTM test in order to reduce variability in the data. All specimens tested were precracked and the largest crack was selected and held to a uniform crack width. The specimen consisted of a 12.7 mm 7-wire prestressing strand in a 180 mm long, 25 mm diameter grouted clear PVC pipe. Only the area immediately around the selected crack was exposed to the saltwater solution (typically between 25 mm and 30 mm). The applied potential, as in the majority of the original ACTM tests,[32] remained at +600 mV_{SCE}. A summary of the grout mixes tested is shown in Table 3.3 and the associated results are shown in Table 3.4. Only specimens of the final specimen configuration, same crack width and with strand from the same reel are included in the summary data.

Table 3.3: Mix Designs for ACTM Tests by Hamilton[15]

Test	*w/c*	*Admixtures*
F	0.40	2.2% cwt Sikament, 19.8 l/m^3 DCI
H	0.40	2.2% cwt Sikament, 5.0 l/m^3 Rheocrete 222*
I	0.38	15% cwt Sikacrete 950DP (replacement), 7.8 ml/kg (c+p)wt WRDA-19**
J	0.40	2.2% cwt Sikament 300SC, 5% cwt Sikacrete 950DP (addition)
K	0.40	2.2% cwt Sikament 300SC
L	0.40	none

*corrosion inhibitor from Master Builders
**superplasticizer from W.R. Grace

Table 3.4: ACTM Results from Hamilton[15]

Test	**Time to Corrosion (hours)***							
	Station						**Average All**	**Average Non Zero**
	1	**2**	**3**	**4**	**5**	**6**		
F	102	2	45	99	126	89	77	77
H	176	170	71	88	nv	156	132	132
I	197	188	150	206	90	213	174	174
J	189	0	123	190	0	233	123	184
K	107	0	138	144	nv	188	115	144
L	144	316	30	320	4	116	155	155

nv = not valid
*non zero stations are those with t_{corr} < 24 hours

Hamilton found increased corrosion protection with the addition of silica fume and reduced protection with the addition of anti-bleed admixture. At an applied potential of +600 mV_{SCE}, the corrosion inhibitor calcium nitrite again had poor performance and actually reduced the time to corrosion significantly.

Additional ACTM studies at The University of Texas at Austin were carried out by Koester for his Master's Thesis entitled, *Evaluation of Cement Grouts for Strand Protection Using Accelerated Corrosion Tests.*[17] The applied potential was changed to +200 mV_{SCE} to examine the effects on grouts containing calcium nitrite. This value should be well within the passive region of the polarization curve for steel.[15] The lowered applied

potential was intended not only to provide a more reliable test for the grouts containing calcium nitrite, but also to reduce data scatter by increasing the time to corrosion. Koester further modified the ACTM by limiting the test to uncracked specimens, and by increasing the area of the specimen exposed to the saltwater. The increase in area was to help counteract the lengthening of the test due to the reduction in applied potential. The final modification involved degreasing the strand with acetone prior to casting the specimens. The present ACTM studies follow the procedure as modified by Koester.[17]

Mix designs tested and results for Koester's series of tests are shown in Tables 3.5 and 3.6. Data scatter relative to previously performed ACTM tests by Hamilton[15] was reduced by the modifications in the ACTM test procedure. Results show an increase in corrosion protection with the reduction of the water cement ratio as well as an indication of poor performance from the grouts containing calcium nitrite. Once again, the calcium nitrite grouts decreased the time to corrosion when compared with plain grouts, even at the lower potentials. This leads to concern about the use of calcium nitrite as a corrosion inhibitor in grout until its poor performance in the ACTM testing is adequately explained.

Table 3.5: Mix Designs for ACTM Tests by Koester[17]

Test	*w/c*	*Admixtures*
1	0.50	none
2	0.40	none
3	0.44	0.9% cwt Intraplast-N (TxDOT grout)
4	0.44	0.9% cwt Intraplast-N, 80 ml/l DCI
5A	0.44	none
5B	0.44	80 ml/l DCI-S (includes retarder)

Table 3.6: ACTM Results from Koester[17]

Test	*# Samples*	$\mu\ t_{corr}$	σ	*COV*
1	14	454	131	0.29
2	9	757	104	0.14
3	12	447	76	0.17
4	12	282	50	0.18
5A	6	536	56	0.10
5B	6	312	73	0.23

T_{corr} = time to corrosion
μ = arithmetic mean
σ = standard deviation
COV = coefficient of variation

3.3 PRESENT ACTM STUDIES

The present ACTM studies focused on grouts that performed well in the fluidity testing phase. Also tested were a 0.40 water-cement ratio plain grout and the TxDOT standard grout to use as a comparison to the results of Koester.[17] Some mix designs were tested twice to investigate repeatability. Strand from two different reels was also tested. Strand A was from the same reel as tested by Koester[17] and strand B was from a reel that was later used for a large-scale beam exposure program funded by the Texas Department of Transportation.[25] The initial, on-reel condition of strand A appeared slightly better than strand B that showed light surface corrosion. All strand for the ACTM tests was cleaned with acetone to remove surface contamination prior to casting. A summary of the grouts tested is shown in Table 3.7.

Table 3.7: Mix Designs for Present ACTM Tests

Test	*w/c*	*Strand*	*Admixtures*
PL-A	0.40	A	none
AB-A1	0.33	A	2% cwt Sikament 300SC
FA-A	0.35	A	30% cwt Fly Ash, 4 ml/kg* Rheobuild 1000
SF-A	0.35	A	15% cwt Sikacrete 950DP, 16 ml/kg Rheobuild 1000
AB-B	0.33	B	2% cwt Sikament 300SC
AB-A2	0.33	A	2% cwt Sikament 300SC
FA-B	0.35	B	30% cwt Fly Ash, 4 ml/kg* Rheobuild 1000
SF-B	0.35	B	15% cwt Sikacrete 950DP, 16 ml/kg Rheobuild 1000
TX-A	0.44	A	TxDOT Standard Grout (0.9% Intraplast-N)
TX-B	0.44	B	TxDOT Standard Grout (0.9% Intraplast-N)

*ml/kg = ml admixture per kg cementitious materials

No further tests were run on grouts containing calcium nitrite. The poor performance of these grouts was initially attributed to high applied potentials, but the performance remained poor at lower potentials in Koester's[17] study. Although the original ACTM report[32] showed better results at lowered potentials, the number of specimens tested was too small to draw definite conclusions about the effectiveness of calcium nitrite. It is possible that the ACTM test may not be well suited for corrosion inhibitors that work by slowing corrosion once it has started instead of causing an increase in the time to corrosion. There is much controversy in this area, and further research would be beneficial before corrosion inhibitors are recommended for use in grouts.

Interestingly, poor performance of a grout containing calcium nitrite was also found in a durability study by West[33] that utilized segmental macrocells. The ASTM standard macrocell was modified to include two match cast segments each with a prestressing strand encased in a grouted duct and with conventional reinforcing bars. The setup simulated post-tensioned segmental precast bridge elements. Variables included duct type, level of segmental compression, grout type, and joint sealant. One specimen from each category was autopsied after 4 years of 2 week long wet-dry cycles of saltwater ponding. Autopsy results revealed light to moderate corrosion of the prestressing strand with pitting for the dry-joint specimen containing calcium nitrite (0.40 w/c) grout. A similar specimen with plain grout (0.40 w/c) showed only light to moderate corrosion with no pitting. At the time the specimens were fabricated, there was little information available on the dosage of calcium nitrite required for use in grout. A dosage similar to what would be used for concrete (19.8 l/m^3) was chosen. This dosage was changed to 80 l/m^3 as suggested by the manufacturer for Koester's[17] grout testing. It is possible that the dosage used in the segmental macrocells was too low for the inhibitor to perform properly. However, the corrosion accelerating effect is worrisome and suggests that further study of this inhibitor is needed before it can be recommended for use in grouts.

3.4 RESULTS

3.4.1 Behavior

The initial behavior for Series AB-A1 is shown in Figure 3.5. This initial rapid reduction in corrosion current was typical in all tests and was helpful in isolating and correcting a faulty station (such as the station showing an initial rise in corrosion current in the figure) early in testing. Plots of initial behavior for all of the grouts tested are found in Appendix A.

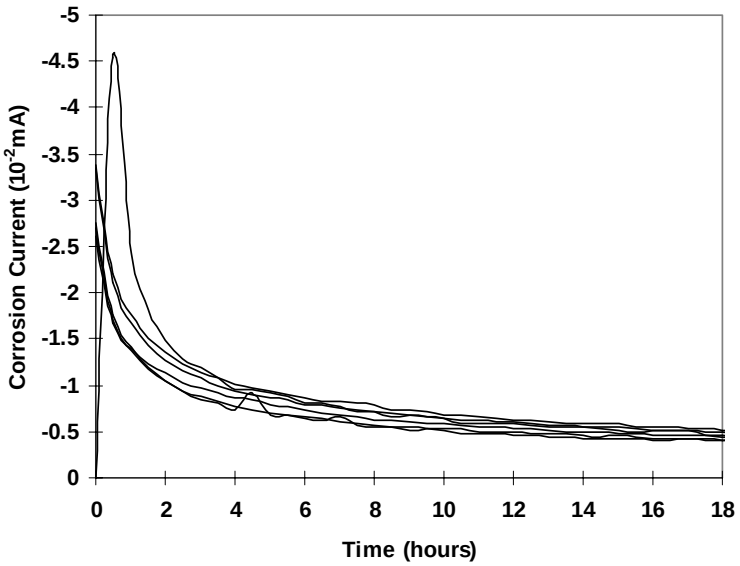

Figure 3.5: Initial Behavior of Corrosion Current with Time (Series AB-A – 0.33 w/c, 2% Anti-bleed)

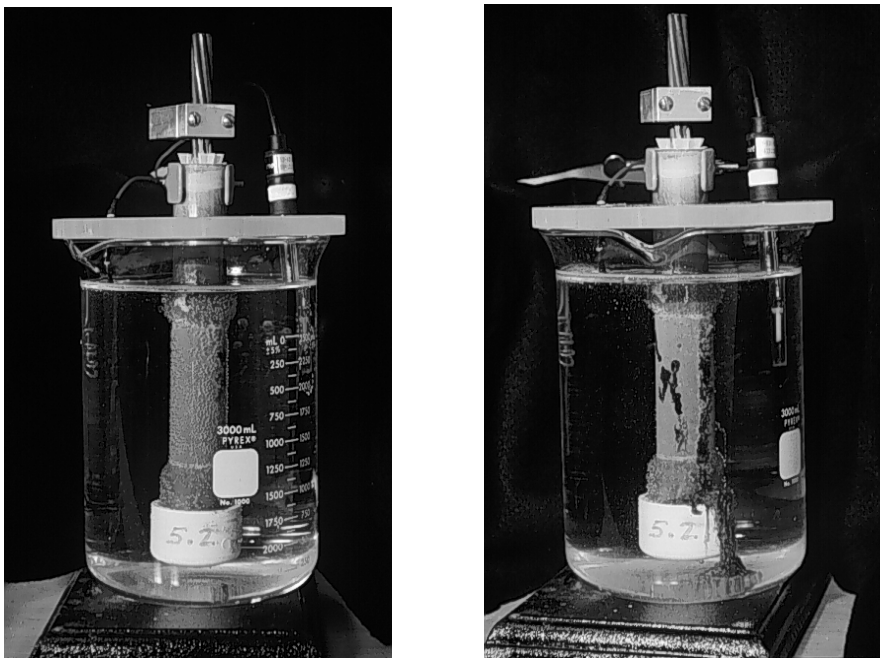

12 Hours after Onset of Corrosion *60 Hours after Onset of Corrosion*

Figure 3.6: Progression of Corrosion

By the first 24 hours, the corrosion current would typically stabilize near zero, until the onset of corrosion when the corrosion current increased by orders of magnitude very rapidly. Soon after a spike in corrosion current, the specimen visibly begins to corrode. Corrosion proceeds rapidly after onset as shown by the photos in Figure 3.6. At a certain time after initiation of corrosion, the current would begin to level off again at a higher plateau. The testing for each specimen continued for approximately four days after the onset of visible corrosion. Figures 3.7 – 3.16 show plots of corrosion current with time for each of the tested grouts. The time to corrosion for each specimen was estimated as the value at which the spike in corrosion current occurred. In some cases,

the spikes were very well defined as seen in the data for Series AB-A1. In other cases, they were somewhat more difficult to pinpoint as seen in the data for Series AB-B. The average time to corrosion for a test series was taken from 6 specimens, except for Series FA-B that had one faulty station during testing.

The slope of the spike in corrosion current can be related to the rate at which a specimen corrodes after the initiation of corrosion. Closer inspection of the slopes of the corrosion current spikes for the series tested revealed as much variation in slope within a series as between two different series. It appears from the data that no conclusions can be made relating the rate of corrosion after initiation for the different grout designs tested.

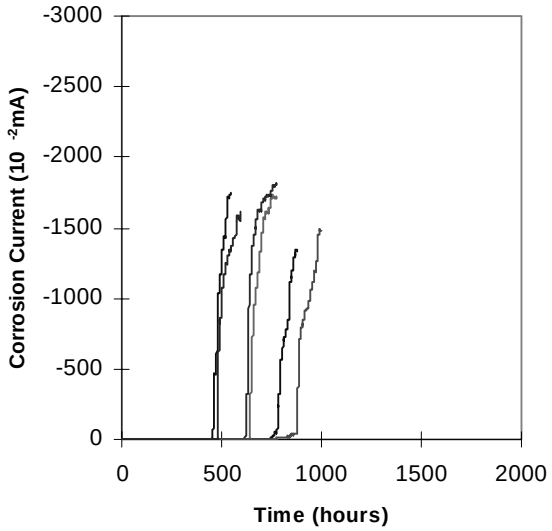

Figure 3.7: Corrosion Current with Time (Series PL-A – 0.40 w/c plain grout, strand A)

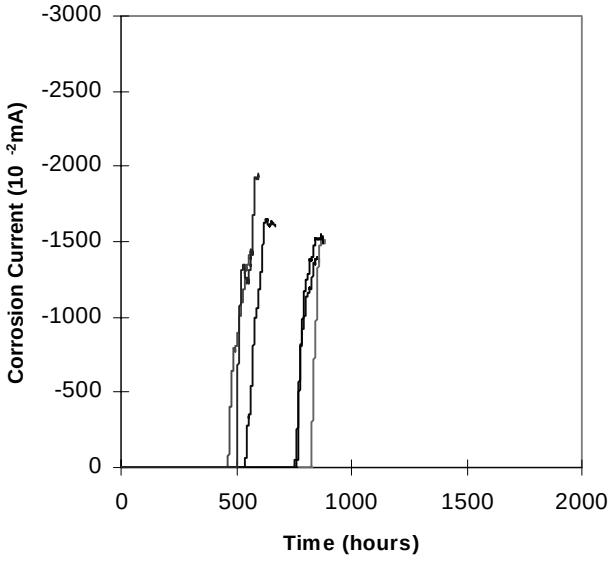

Figure 3.8: Corrosion Current with Time (Series AB-A1 – 0.33 w/c, 2% anti-bleed, strand A)

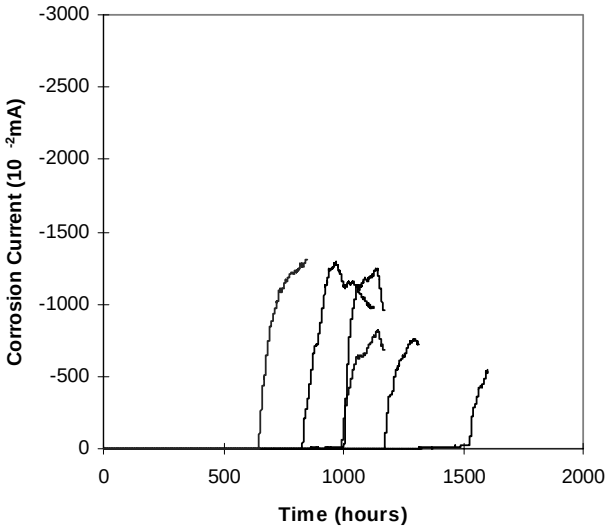

Figure 3.9: Corrosion Current with Time
(Series FA-A – 0.35 w/c, 30% fly ash 4 ml/kg superplasticizer, strand A)

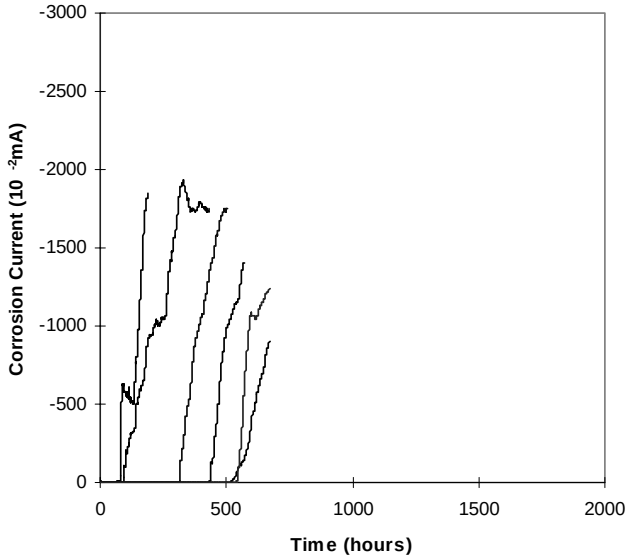

Figure 3.10: Corrosion Current with Time
(Series SF-A – 0.35 w/c, 15% silica fume, 16 ml/kg superplasticizer, strand A)

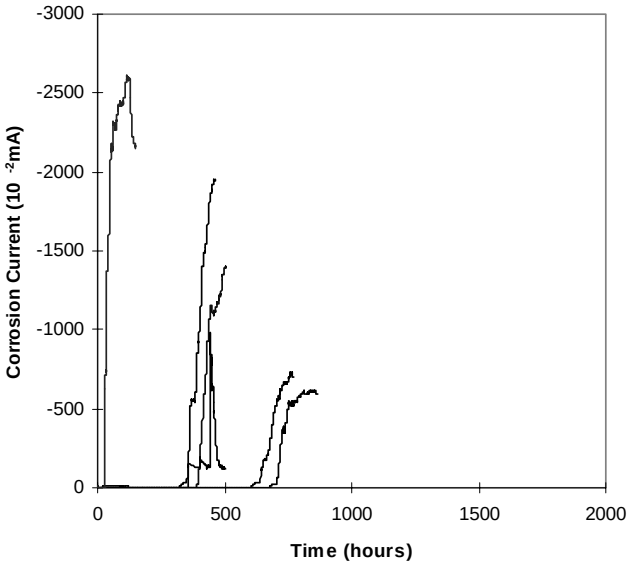

Figure 3.11: Corrosion Current with Time
(Series AB-B – 0.33 w/c, 2% anti-bleed, strand B)

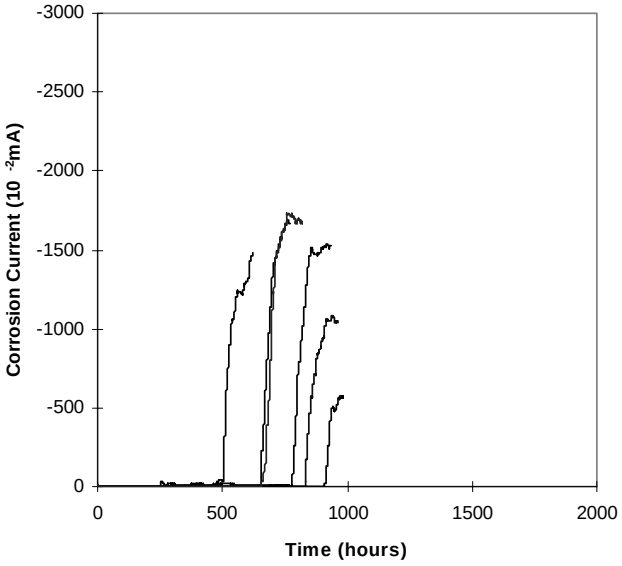

Figure 3.12: Corrosion Current with Time
(Series AB-A2 – 0.33 w/c, 2% anti-bleed, strand A)

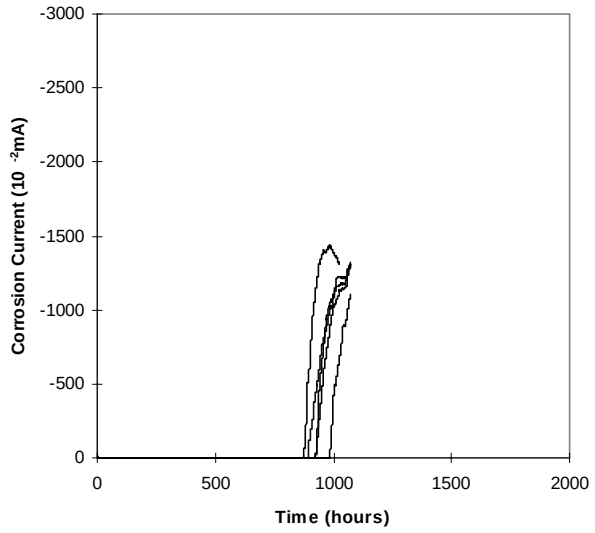

Figure 3.13: Corrosion Current with Time
(Series FA-B – 0.35 w/c, 30% fly ash, 4 ml/kg superplasticizer, strand B)

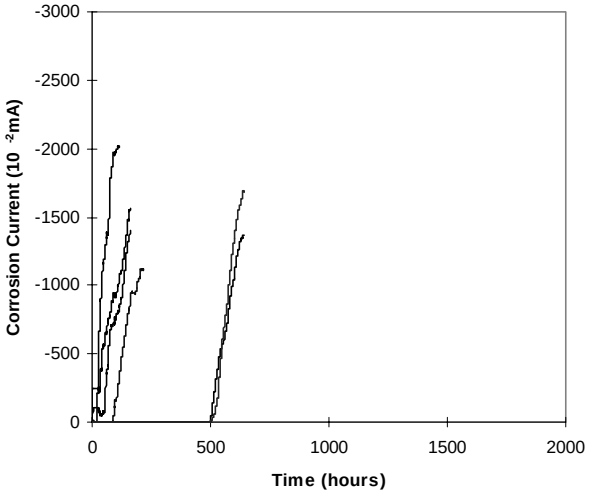

Figure 3.14: Corrosion Current with Time
(Series SF-B – 0.35 w/c, 15% silica fume, 16 ml/kg superplasticizer, strand B)

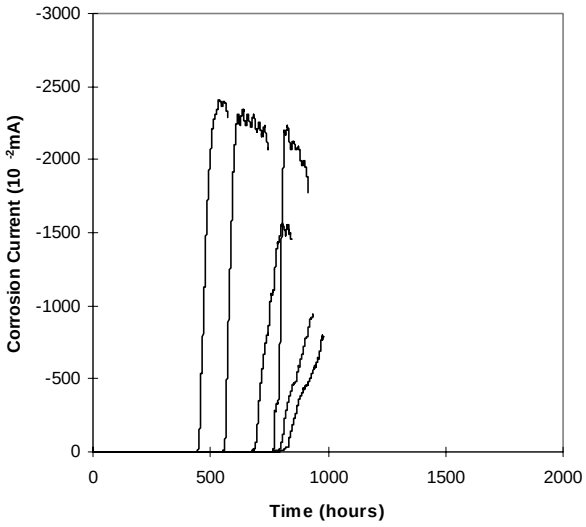

Figure 3.15: Corrosion Current with Time
(Series TX-A – 0.44 w/c, 0.9% expansive agent, strand A)

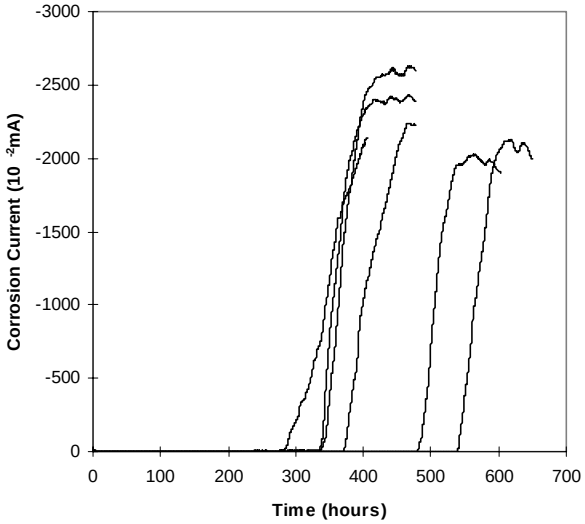

Figure 3.16: Corrosion Current with Time
(Series TX-B – 0.44 w/c, 0.9% expansive agent, strand B)

3.4.2 Free Corrosion Potential

Plots comparing the initial corrosion current (i_{corr}) and the free corrosion potential (free E_{corr}) for each series are given in Appendix B. No definite trends exist between i_{corr} and the free E_{corr}. A comparison of the initial corrosion current at time t=0 can not be made between the series because the initial corrosion current measured is not taken at exactly the same time for each series. The data logger records values each half-hour and specimens were connected at different times during the first 15 minutes prior to the initial reading.

Plots of free E_{corr} and the time to corrosion (t_{corr}) are given in Appendix C for each series. A comparison of the average free E_{corr} and average t_{corr} between the test series is shown in Figure 3.17. There appears to be poor correlation between the average free corrosion potential and the average time to corrosion. Koester[17] found some evidence of correlation in his grout studies that may suggest that grouts with more negative average free corrosion potentials will tend to have shorter average times to corrosion. However, the correlation is not strong enough to support comparing grouts solely on their free corrosion potential values. Figure 3.18 more clearly illustrates the lack of correlation between the free corrosion potential and the average time to corrosion.

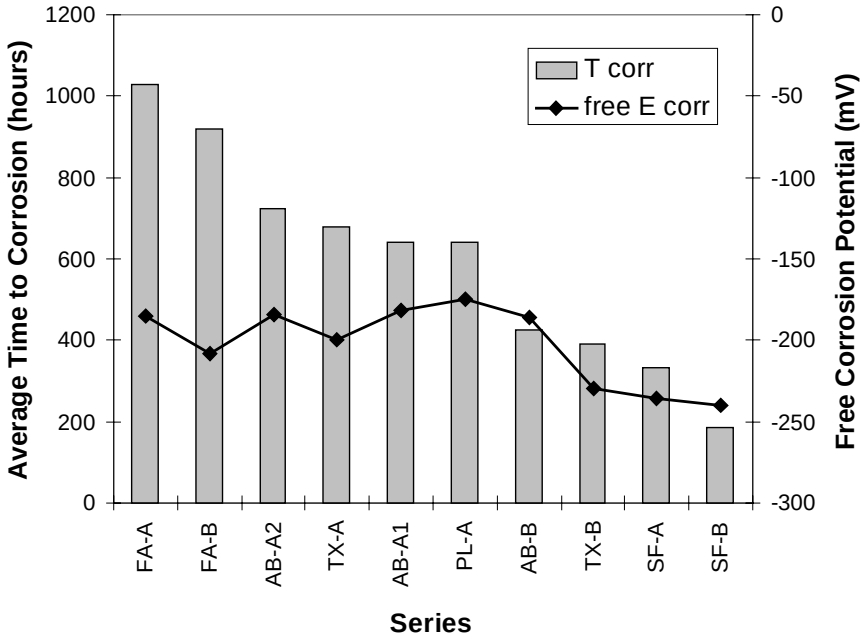

Figure 3.17: Comparison of Free Corrosion Potential and Average Time to Corrosion for All Test Series

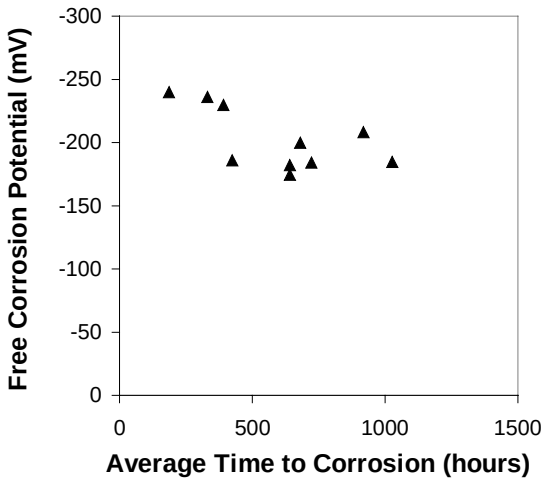

Figure 3.18: Correlation between Free Corrosion Potential and Average Time to Corrosion

3.4.3 Time to Corrosion Comparisons

Table 3.8 shows the statistical results for the grouts tested in the present series. Figure 3.19 gives a corresponding plot of the data with bar lengths indicating two standard deviations on each side of the mean. Although standard deviations for certain mixes were much larger than for others, repeatability between tests of the same design was quite good. This repeatability was evident not only for tests repeated in the present study, but also between the present study and the values found by Koester.[17]

Table 3.8: Results from Present ACTM Tests

Test	*# Samples*	$\mu\ t_{corr}$	σ	*COV*
PL-A	6	641	165	0.26
AB-A1	6	642	157	0.24
FA-A	6	1028	302	0.29
SF-A	6	332	206	0.62
AB-B	6	424	245	0.58
AB-A2	6	723	147	0.20
FA-B	5	920	42	0.05
SF-B	6	185	245	1.32
TX-A	6	680	149	0.22
TX-B	6	391	98	0.25

T_{corr} = time to corrosion
μ = arithmetic mean
σ = standard deviation
COV = coefficient of variation

A comparison of grout performance is most easily seen in Figure 3.20 that includes data from the present study and from Koester's study[17] with values from the same mix designs averaged together. Since these are the results of an accelerated corrosion test, the actual times shown are not intended to directly relate to actual service life. The test is used as a relative comparison between different grout types.

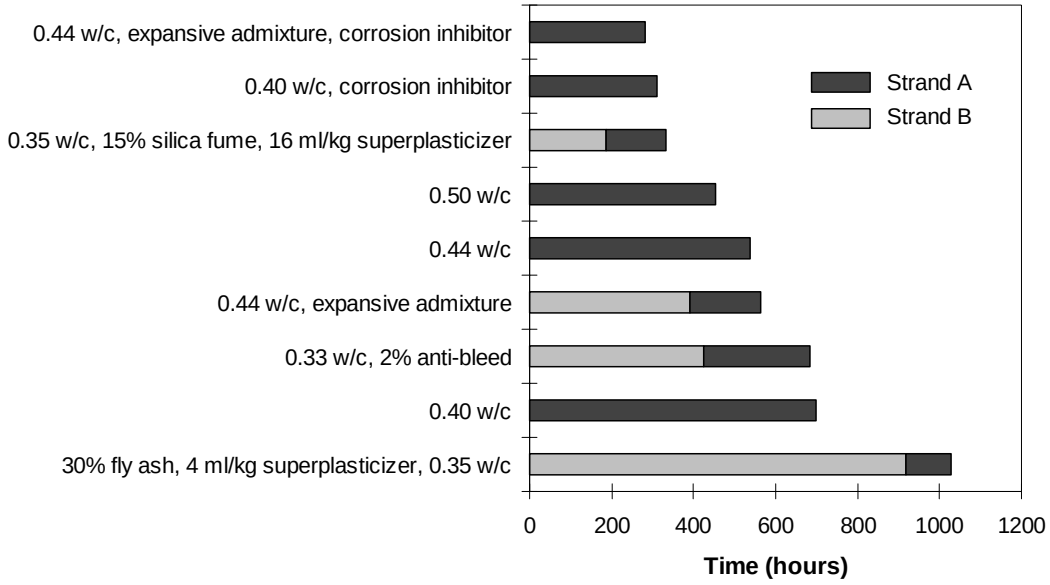

Figure 3.19: Comparison of ACTM Average Times to Corrosion

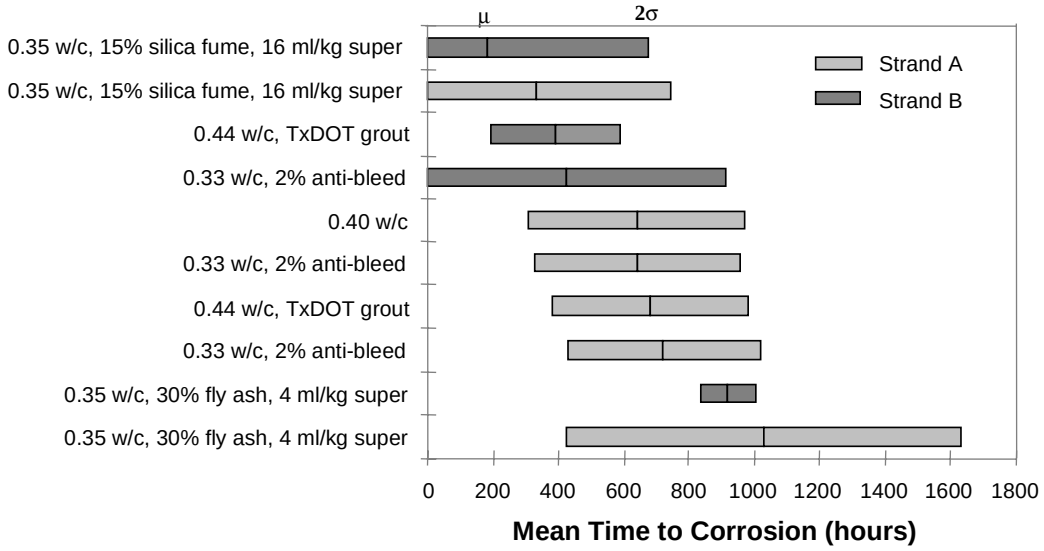

Figure 3.20: ACTM Grout Performance
(Summarized Results of Schokker and Koester[17])

The longer bars in the figure indicate longer times to corrosion and therefore better corrosion protection. Strands from the two different reels are included for comparison. The consistently longer values for Strand A show the importance of using the same strand throughout a test series. The addition of fly ash to the mix gave the highest time to corrosion with over 40% improvement in corrosion protection over the next best grout. The mix containing anti-bleed admixture also tested well. Although anti-bleed admixture has been known to reduce time to corrosion,[15] the very low water-cement ratio of 0.33 allowed this mix to perform favorably. This mix was the only grout design from the current tests that passed all of the fresh property tests including the pressurized bleed test. The beneficial effect of lowering water-cement ratio is evident in this plot through comparison of the plain grouts with 0.40, 0.44, and 0.50 water-cement ratios.

Most of the grouts containing chemical admixtures did not perform well. These included the TxDOT grout that contains an expansive admixture / superplasticizer, a silica fume grout with superplasticizer, and grouts

containing the corrosion inhibitor calcium nitrite. The poor performance of the silica fume grout is likely due to the large amount of superplasticizer that was necessary for this grout to maintain fluidity at a water-cement ratio of 0.35. Silica fume is likely to be more beneficial in smaller percentages of replacement,[34] but the replacement percentage of 15% of the cement weight was chosen to correspond with the suggestions of 15-25% replacement silica fume in the draft of the PTI grouting specifications available at the time of testing. The latest draft of the specifications recommends 5-15%. It is also possible that silica fume is more applicable at higher water-cement ratios due to the large amount of superplasticizer necessary to maintain fluidity at low water-cement ratios. The poor performance of the grout containing the corrosion inhibitor calcium nitrite stands out in the figure. A discussion of the problems with this grout was included in previous sections.

It is evident from the data that a grout that combines low permeability and minimal chemical admixtures gives the best corrosion performance in the ACTM tests.

CHAPTER 4

LARGE SCALE DUCT TESTING

Grouts that performed favorably in the fresh property test phase and the accelerated corrosion test phase were tested in a large scale draped parabolic duct to simulate field conditions. This test used a clear duct to investigate grout flow along the duct and strand along with the formation of bleed water lenses due to changes in duct elevation. The workability of the grout during pumping was also observed.

4.1 TEST SETUP AND PROCEDURE

A clear vinyl flexible tube (38 mm inside diameter) with a bundle of three untensioned 13mm, 7 wire prestressing strands was used to simulate conditions in a post-tensioning duct. A three-strand tendon was chosen since it might promote water movement or wicking along the length of the strand bundle. The three-strand bundle provided a realistic steel area to duct area ratio. The duct was connected in a parabolic shape to a wooden frame with dimensions as shown in Figure 4.1. The grouted duct is shown in Figure 4.2.

Grouting procedures followed those recommended by the Post Tensioning Institute.[23] Vents were located at the crowns and slightly downstream of the main crown. A single crown vent is not sufficient in ducts with changes in elevation since air can be trapped in the descending limb.[11] The duct was grouted from the low point on the right end. During grouting, vents were closed in order from the inlet to the outlet of the duct with the exception of the intermediate crest where the downstream vent was closed prior to the corresponding crown vent. Each vent was closed after a steady stream of grout was ejected with a volume greater than that of the duct between the vent and the previous vent. A close-up picture of the main crown vent is shown in Figure 4.3.

After grouting, the duct was sealed and allowed to set. The hardened grouted duct was autopsied by removing approximately 50 mm slices from critical locations. The slice locations are marked with X symbols in Figure 4.1, and a diagram of a typical slice is shown in Figure 4.4. In order to minimize disruption of the slice, a large section of the duct that contained the slice was removed directly from the frame. The slice was then cut from this larger section after removal from the frame. The slices were evaluated for area voids and perimeter voids as defined in the figure. Both forms of void parameters are necessary since a void coinciding with a tendon is likely to be more critical than a void that does not expose the tendon.

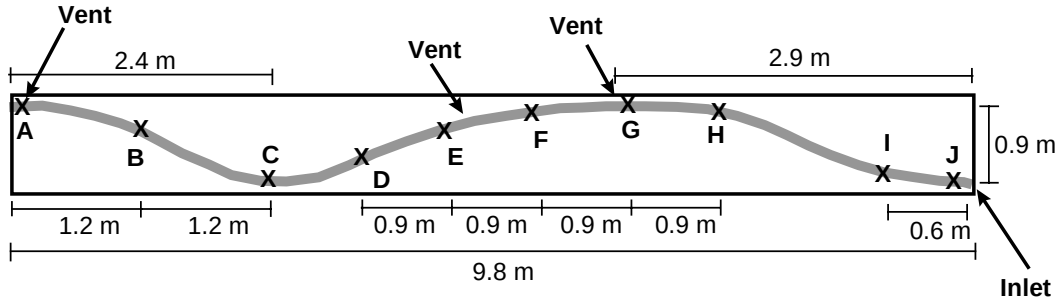

Figure 4.1: Duct Frame Dimensions and Autopsy Cut Locations

Figure 4.2: Grouted Duct

Figure 4.3: Main Crown Vent

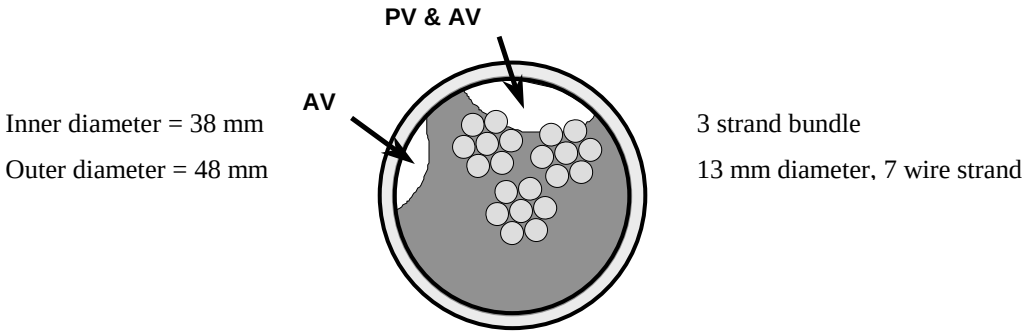

PV = perimeter voids = exposed strand perimeter / total strand perimeter

AV = area voids = area of voids in grout slice / (area of duct – area of strands)

Figure 4.4: Typical Grouted Duct Slice

4.2 RESULTS

Three grout mix designs were tested in the draped duct. The first grout tested was a grout with a 0.33 water-cement ratio and 2% anti-bleed admixture. This grout had the best performance of grouts tested in the fresh property tests and had good performance in the accelerated corrosion tests. The grout was very workable if kept agitated, and no voids or bleed water were noticed in the duct at any time. Autopsy slices revealed no voids along the entire length of the duct.

The next grout tested was a 30% fly ash grout with a 0.35 water-cement ratio that had the best performance in the accelerated corrosion tests. This grout was very workable and no voids were observed during pumping. Approximately 10 minutes after pumping, a long, very thin void was observed near the intermediate crest. Within 24 hours the water in the void had reabsorbed and the void was no longer noticeable. Upon autopsy, no voids were found in any of the duct slices.

The standard TxDOT grout was also tested in the parabolic duct as a comparison to the other grouts. The original test of this grout was unusable. Autopsy slices revealed that the grout never fully set and the grout crumbled when touched. The likely cause was use of Intraplast-N admixture that was past its expiration date. The test was successfully rerun with fresh Intraplast-N. The grout was very workable and easy to pump. Immediately after pumping, bleed water was visible in the duct. Bubbles traveled to the intermediate crest where a large void pocket was formed. The bubbles and forming of the void are shown in Figures 4.5 and 4.6. After 24 hours, the bleed water had reabsorbed and a large void remained at the intermediate crest.

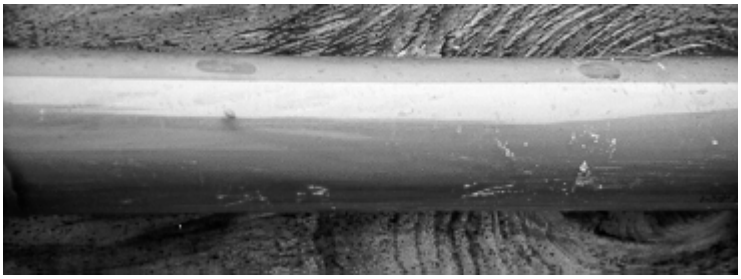

Figure 4.5: TxDOT Grout – Bubbles Traveling Toward Intermediate Crest

Figure 4.6: Beginning of Void Formation at Intermediate Crest

A comparison of autopsy slices at the intermediate crest for each of the three grouts tested in the large-scale test is shown in Figure 4.7. The anti-bleed grout and fly ash grout have no noticeable voids, while the TxDOT grout has a large void that exposes the tendon. The bleed behavior of the TxDOT standard grout and the fly ash grout shows the importance of field testing. These two grouts had the same performance in the standard bleed test, but field testing showed significantly better bleed performance from the fly ash grout.

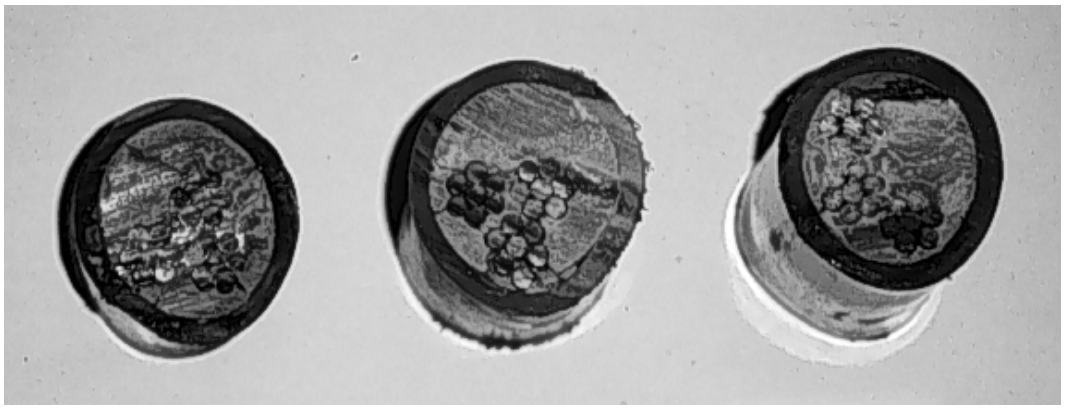

Anti-bleed Grout	*Fly Ash Grout*	*TxDOT Standard Grout*
(0.33 w/c, 2% Sikament)	*(0.35 w/c, 30% Fly Ash, 4 ml/kg Rheobuild)*	*(0.44 w/c, 0.9% Intraplast-N)*

Figure 4.7: Comparison of Slices from the Intermediate Crest

An interesting comparison can also be made between the flow characteristics of each grout during pumping. The anti-bleed grout filled the duct completely as it moved along the length of the duct similar to the grout shown in Figure 4.8(a). This flow pattern is conducive to complete filling of the duct without leaving pockets

of trapped air as long as the grout is suitably workable,[11] although using a grout with this type of flow should not be a substitute for proper venting. The TxDOT standard grout followed a more "loose" flow pattern similar to the drawing in Figure 4.8(c). This type of flow is more likely to result in the formation of air pockets since the grout only fills the lower half of the duct initially. This grout may become less fluid by the time another stream of grout pushes through to fill the upper half of the duct. The situation is further complicated by a parabolic shaped duct that may fill more quickly at the lower points in the duct. It should be noted, however, that in the present study, proper venting and procedure (along with the ability to see void formation through the clear duct) eliminated trapped air pockets and the voids found in the TxDOT grout were due to bleed water rising to the intermediate crest. The fly ash grout tested exhibited a flow pattern as shown in Figure 4.8 (b).

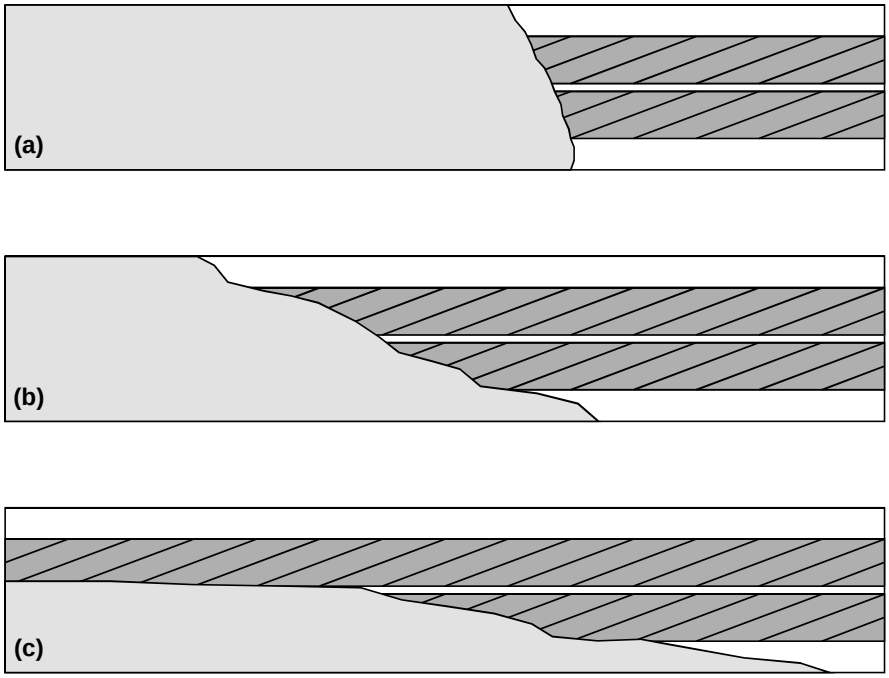

Figure 4.8: Types of Grout Flow Patterns

CHAPTER 5

RECOMMENDATIONS

A summary of the results is shown in Table 5.1 for the grout designs tested in all three phases. Workability is important for any grout considered, and all three mixes tested had adequate fluidity. The fluidity values shown in Table 5.1 are those recorded during the large scale duct testing phase. These values are reduced from those originally found in the fluidity testing phase due to cooler temperatures during the parabolic duct testing.

Bleed resistance is a desirable property, but the degree of bleed resistance necessary depends on the situation. For ducts with little change in elevation, bleed resistance under large values of pressure is unnecessary. Since the anti-bleed admixture that is needed for pressurized bleed resistance tends to decrease corrosion protection properties, it may be a beneficial tradeoff in many horizontal structural elements to have more corrosion protection with less bleed resistance. However, if bleed may be a problem, such as in structural members with large vertical rises, the anti-bleed admixture should be included so that voids do not result from bleed lense formation.

All three mixes tested had adequate standard bleed resistance, but only the anti-bleed grout had good pressurized bleed resistance. The fly ash grout had excellent corrosion performance with over 40% increase in corrosion protection over the next best grout. The anti-bleed grout had good corrosion protection with an average time to corrosion similar to that of a 0.40 water-cement ratio plain grout. The TxDOT standard grout had average corrosion protection properties with an average time to corrosion below that of the 0.40 water-cement ratio plain grout. Performance under simulated field conditions was excellent for both the anti-bleed grout and the fly ash grout. The standard TxDOT grout performed poorly under simulated field conditions by leaving a large void that exposed the post-tensioning tendon.

Table 5.1: Summary of Grout Testing Phases

Grout Design	*Fluidity (sec)*	*Standard Bleed (%)*	*Pressure Bleed (%)*	*Mean t_{corr}* (hrs)*	*Area Voids (%)*	*Perimeter Voids (%)*
Anti-bleed (mix #19)**	20	0	1.9	683	0	0
Fly ash (mix #8)	17	0.6	Instant bleed	1028	0	0
TxDOT (mix #31)	19	0.6	Instant bleed	447	16	8

* t_{corr} = time to corrosion
** mix number refers to Table 3.2

5.1 RECOMMENDED GROUTS

- **0.35 water-cement ratio, 30% cement weight replacement fly ash (class C), and 4 ml/kg superplasticizer**

This grout is recommended for situations requiring a high resistance to corrosion without extreme bleed conditions (vertical rise of less than 1 meter). This grout may also be appropriate for larger vertical rises (1-5 m), but field-testing should be performed on a case by case basis. The superplasticizer dosage may need to be adjusted slightly depending on conditions (and brand used), but the dosage should be kept at a minimum (while attaining the necessary workability) to ensure maximum corrosion protection. The superplasticizer tested was Rheobuild 1000 from Master Builders.

- **0.33 water-cement ratio, 2% anti-bleed admixture**

This grout is recommended for situations requiring a high resistance to bleed (vertical rises up to 38 m) along with good corrosion protection. The maximum vertical rise recommended was based on results of the Gelman pressure test. The grout was not actually tested in a 38 m vertical rise. The anti-bleed admixture dosage may need to be adjusted slightly depending on conditions (and brand used), but the dosage should be kept at a minimum (while attaining the necessary workability) to ensure maximum corrosion protection. The anti-bleed admixture tested was Sikament 300SC from Sika Corporation.

5.2 SELECTING GROUT DESIGNS

For special conditions not covered in Section 5.1, grout designs should be tested for adequate fresh properties, hardened properties, corrosion protection properties, and should be evaluated under simulated field conditions before being used in a structure. Negative interactions between admixtures are possible. A summary of guidelines for selecting grout designs is as follows:

Use a low water-cement ration (0.35 or below preferred).

Minimize chemical admixtures which can be detrimental to the corrosion protection properties of the grout (maintain desired properties such as fluidity or bleed reduction while keeping admixture dosages at a minimum).

Avoid calcium nitrite based corrosion inhibitors until their poor performance in the accelerated corrosion tests is adequately explained. Other types of corrosion inhibitors should be tested for their corrosion protection properties in grout before they are used.

Utilize thixotropic mixes when conditions warrant (large vertical rises).

Pozzolan addition can produce many beneficial properties (fly ash may be more useful than silica fume due to fluidity concerns).

If the ACTM (Accelerated Corrosion Testing Method) is used to evaluate the corrosion protection properties of a grout, the grout in question should be tested along with at least one base grout (such as a 0.40 w/c plain grout). It is also advisable to test one of the two recommended grouts with the new grout as a comparison. At least six specimens should be tested for each grout type to find an average time to corrosion. Materials should be consistent for each grout batch (distilled water, cement from the same batch, strand from the same spool) because inconsistency may cause significant variances in the results.

5.3 GROUTING PROCEDURE

Good grouting practice is critical to obtaining a corrosion resistant post-tensioned structure. Grouts are complex fluids that must fill the complex area left between the post-tensioning tendon and the duct. Proper venting and continuous grouting are necessary to avoid voids in the grouted duct, and knowledgeable grouting crews can greatly increase the likelihood of a properly grouted duct. The Post Tensioning Institute's *Guide Specification for Grouting of Post-Tensioned Structures*[23] provides detailed description of good grouting practice.

Grouting is a critical component of the construction of post-tensioned structures as it is the last line of defense against corrosion of the high strength steel tendon. An additional challenge to grouting is that the grout crew is unable to see the duct and the progress of the grout. Even in controlled testing, problems can occur with complete filling of the duct as evidenced by Sprinkel's testing on silica fume grouts[30] that led him to suggest the need for an experienced grout inspector on site. New grout designs must be tested before use in the actual structure to ensure adequate fresh properties and to evaluate the effects of admixtures on corrosion protection properties as well as possible negative interactions between admixtures.

CHAPTER 6

SUMMARY

The cement grout injected into the tendons in post-tensioned bridge structures has the important dual role of providing bond between the strands or bars and the concrete, as well as providing corrosion protection to the prestressing strands (or bars). An optimum grout combines good corrosion protection with desirable fresh properties so that the ducts can be completely filled with ordinary grouting techniques. Numerous grouts were tested in three phases of testing to develop a high performance grout for corrosion protection. The testing phases included fresh property tests, accelerated corrosion tests, and a large-scale clear draped parabolic duct test that allowed observation of the grout under simulated field conditions. Observations and conclusions from each of the three test phases are given below along with the recommended grouts.

6.1 FRESH PROPERTY TESTS

- Fluidity
  - Increased with the addition of fly ash
  - Decreased with the addition of silica fume
  - Required the use of superplasticizer at low water-cement ratios
- Standard bleed
  - Reduced with the addition of fly ash or silica fume
  - Increased with the addition of superplasticizer
- Bleed under pressure
  - Required an anti-bleed admixture to pass this test

6.2 ACCELERATED CORROSION TESTS

- Corrosion protection increases with lowered water-cement ratio.
- Corrosion protection decreases with the addition of chemical admixtures including a calcium nitrite corrosion inhibitor.
- A 30% fly ash grout with a 0.35 water-cement ratio had excellent performance (over 40% increase in average time to corrosion compared to a 0.40 water-cement ratio plain grout) and is recommended for use in most horizontal applications.
- A 2% anti-bleed grout with a 0.33 water-cement ratio had good performance (average time to corrosion was similar to that of a 0.40 water-cement ratio plain grout) and is recommended for use in most high bleed vertical applications.
- The standard TxDOT grout had below average performance (average time to corrosion was lower than for a plain grout at the same water-cement ratio).
- Using prestressing strand from different spools can alter the test results. When comparing grout designs, the strand used should be consistent among all grouts.

6.3 LARGE-SCALE DUCT TESTS

- The 2% anti-bleed grout with a 0.33 water-cement ratio had excellent performance (no voids were found during pumping or during autopsy).
- The 30% fly ash grout with a 0.35 water-cement ratio had good performance (a thin void was noticed immediately after pumping, but the bleed water reabsorbed and no voids were found during autopsy).

- The TxDOT standard grout had poor performance (voids were observed forming during pumping and autopsy revealed a large void at the intermediate crest that exposed the prestressing strand).

6.4 IMPLEMENTATION RECOMMENDATIONS

6.4.1 Post-Tensioned Tendons with Small Rises

For post-tensioned tendons with a rise less than 1-5 meter, the present TxDOT standard grout should be replaced by:

- **0.35 water-cement ratio, 30% cement weight replacement fly ash (class C), and 4 ml/kg superplasticizer (Rheobuild 1000)**

This grout is recommended for situations requiring a high resistance to corrosion without extreme bleed conditions (vertical rise of less than 1 meter). This grout may also be appropriate for larger vertical rises (1-5 m), but field testing should be performed on a case by case basis.

6.4.2 Post-Tensioned Tendons with Large Rises

For post-tensioned tendons with large rises (5-38 m), the present TxDOT standard grout should be replaced by:

- **0.33 water-cement ratio, 2% anti-bleed admixture (Sikament 300SC)**

This grout is recommended for situations requiring a high resistance to bleed (vertical rises up to 38 m) along with good corrosion protection. The maximum vertical rise recommended was based on results of the Gelman pressure test. The grout was not actually tested in a 38 m vertical rise.

6.4.3 Recommendations

The TxDOT specification requirements for post-tensioning grouting procedures should be reviewed and revised as required to conform to the Post-Tensioning Institute's *Guide Specification for Grouting of Post-Tensioned Structures*[23] and the British Working Party of the Concrete Society's *Durable Bonded Post-Tensioning Bridges.*[35] The latter contains important information for the training of grouting technicians that is often overlooked.

APPENDIX A

ACTM INITIAL BEHAVIOR PLOTS

Figures A1-A10 show the initial behavior of all grouts tested in the accelerated corrosion testing phase. Typical behavior, as shown in Figure A1, is a sharp reduction in corrosion current shortly after the beginning of testing. These plots are helpful in determining a faulty station early in testing. Those figures showing a rise in current after the first hour of testing indicate the onset of corrosion early in testing.

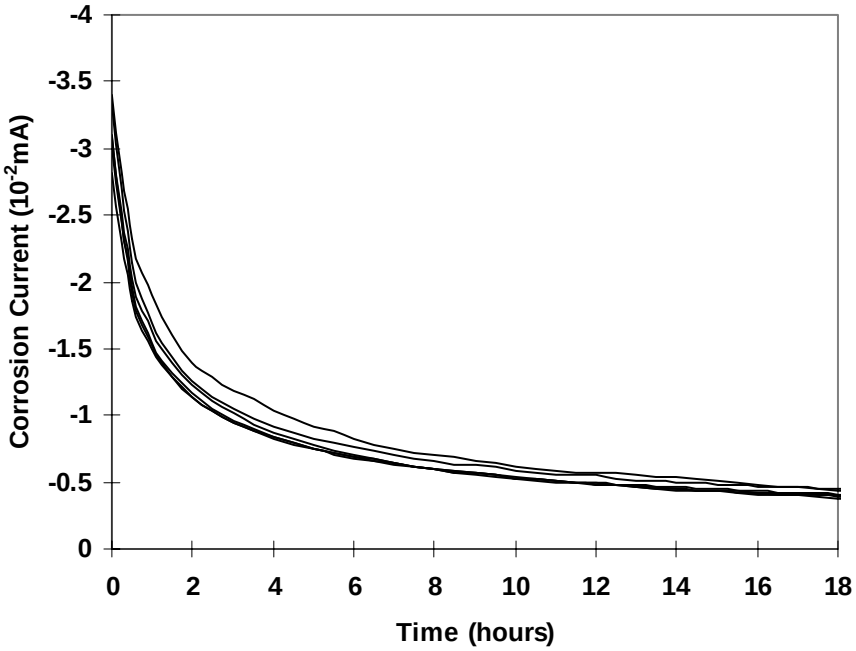

Figure A1: Initial Behavior of Corrosion Current with Time (Series PL-A – 0.40 w/c, plain grout)

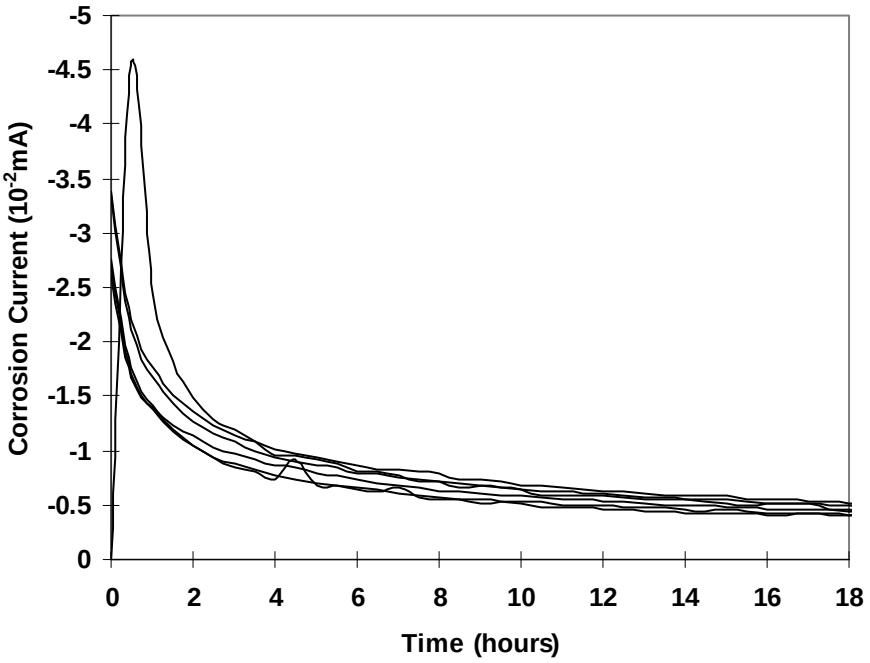

Figure A2: Initial Behavior of Corrosion Current with Time
(Series AB-A1 – 0.33 w/c, 2% anti-bleed, strand A)

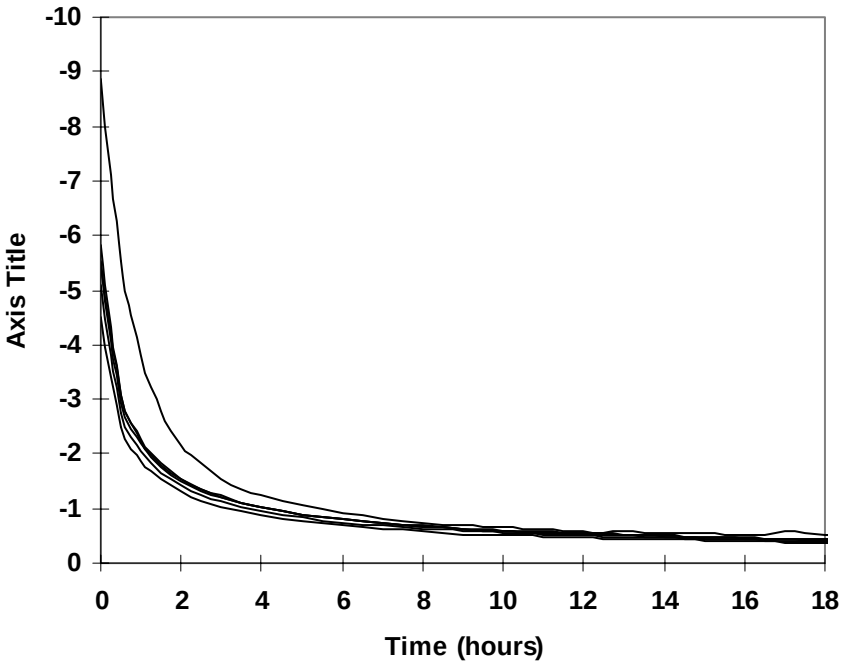

Figure A3: Initial Behavior of Corrosion Current with Time
(Series FA-A – 0.35 w/c, 30% fly ash, 4 ml/kg superplasticizer, strand B)

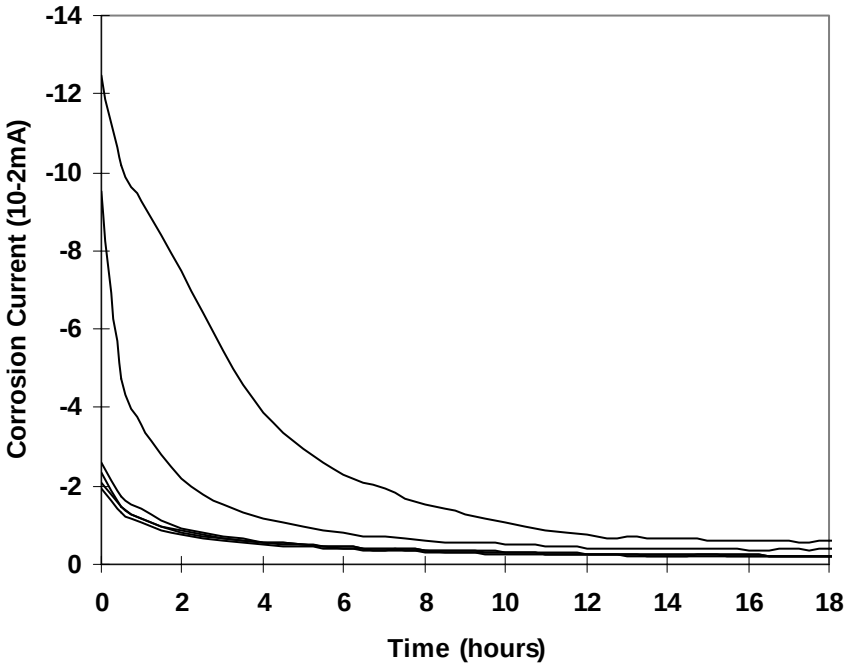

Figure A4: Initial Behavior of Corrosion Current with Time
(Series SF-A – 0.35 w/c, 15% silica fume, 16 ml/kg superplasticizer, Strand A)

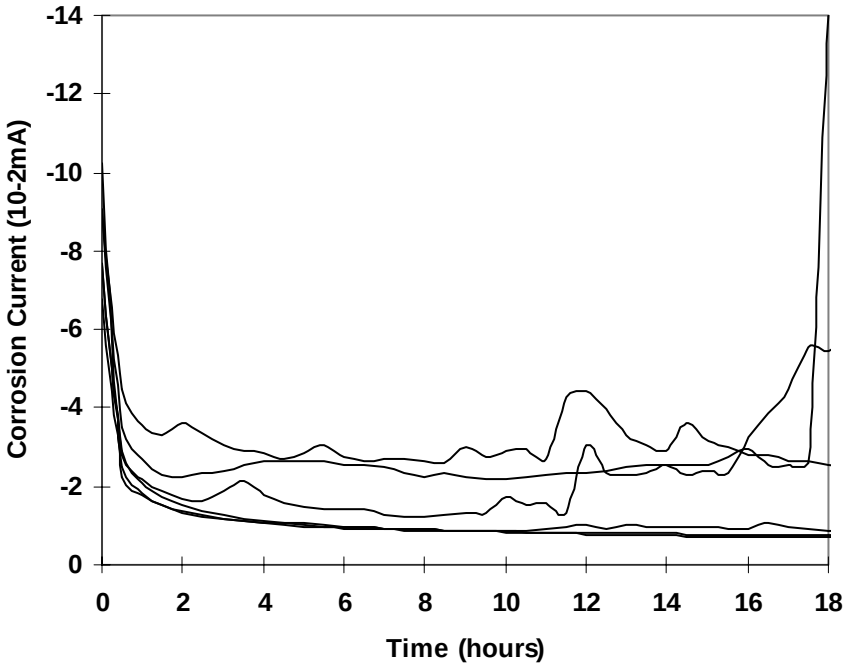

Figure A5: Initial Behavior of Corrosion Current with Time
(Series AB-B – 0.33 w/c, 2% anti-bleed, Strand B)

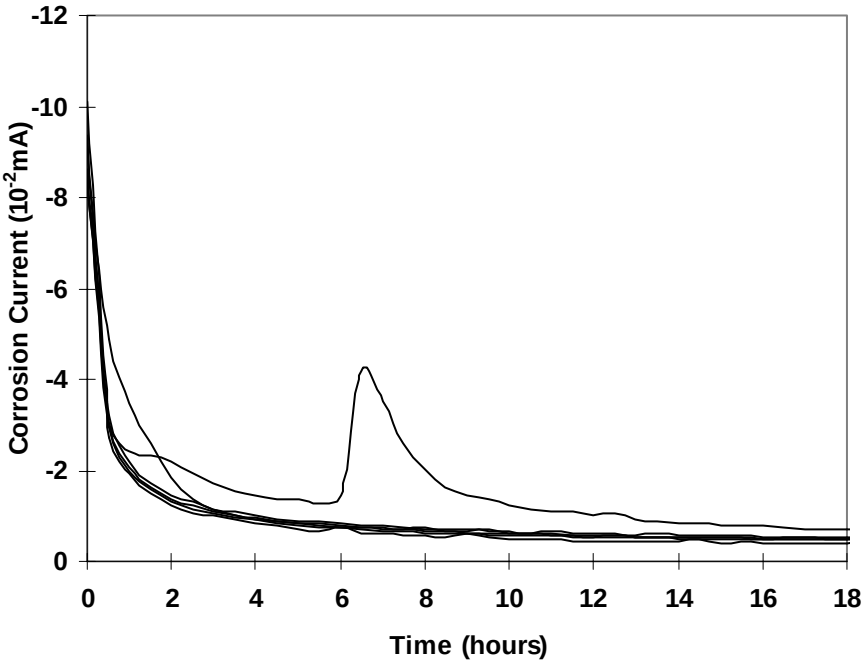

Figure A6: Initial Behavior of Corrosion Current with Time
(Series AB-A2 – 0.33 w/c, 2% anti-bleed, Strand A)

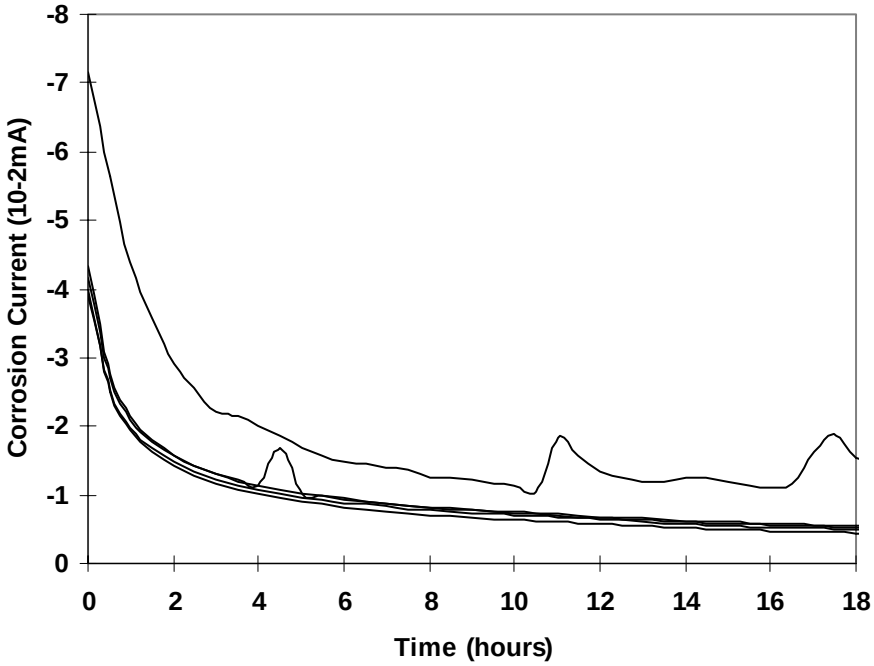

Figure A7: Initial Behavior of Corrosion Current with Time
(Series FA-B – 0.35 w/c, 30% fly ash, 4 ml/kg superplasticizer, Strand B)

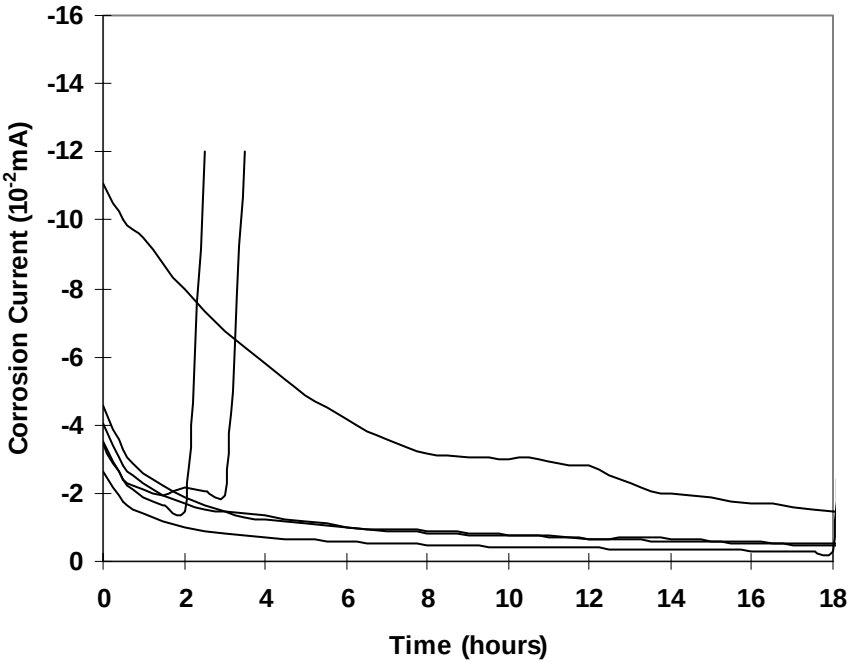

Figure A8: Initial Behavior of Corrosion Current with Time
(Series SF-B – 0.35 w/c, 15% silica fume, 16 ml/kg superplasticizer, Strand B)

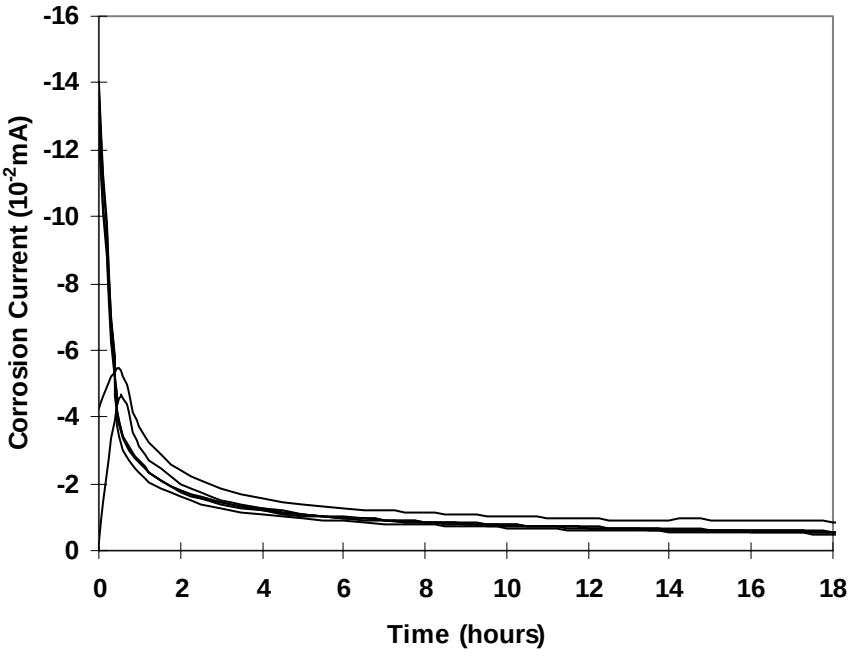

Figure A9: Initial Behavior of Corrosion Current with Time
(Series TX-A – 0.44 w/c, 0.9% expansive admixture)

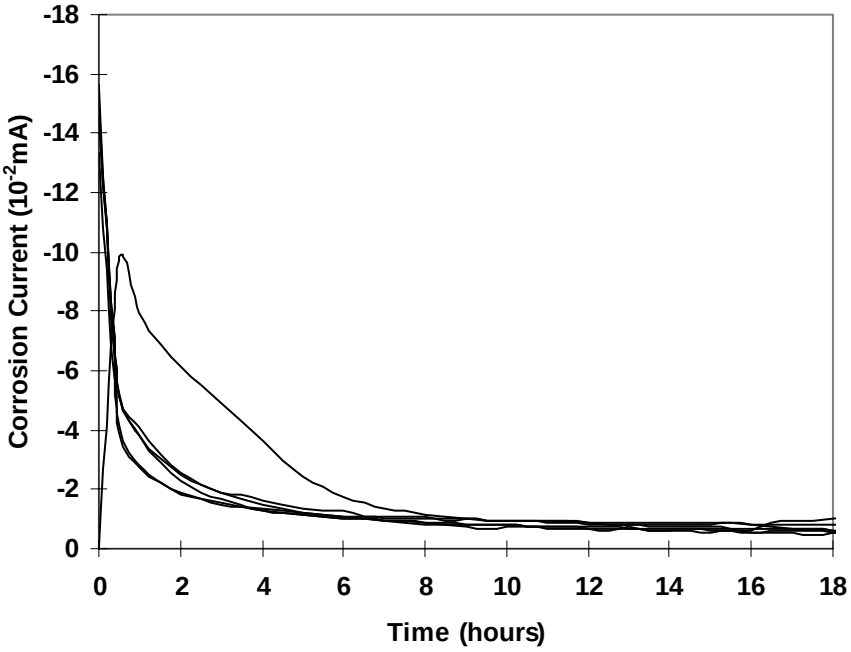

Figure A10: Initial Behavior of Corrosion Current with Time (Series TX-B – 0.44 w/c, 0.9% expansive admixture)

APPENDIX B

INITIAL CORROSION CURRENT VERSUS FREE CORROSION POTENTIAL PLOTS

Figures B1-B10 give a comparison of the initial corrosion current (I_{corr}) and the free corrosion potential (free E_{corr}) for each of the grouts tested in the accelerated corrosion testing phase. There are no definite trends between i_{corr} and the free E_{corr}. The data logger records values each half hour, and specimens were connected at different times during the first 15 minutes prior to the initial reading. Therefore, a comparison of the initial corrosion current at time t=0 cannot be made between the series because the initial corrosion current measured is not taken at exactly at the same time for each series. Specimen 2 in Figure B2 and Specimen 3 in Figure B10 show faulty stations that were corrected immediately after the initiation of testing.

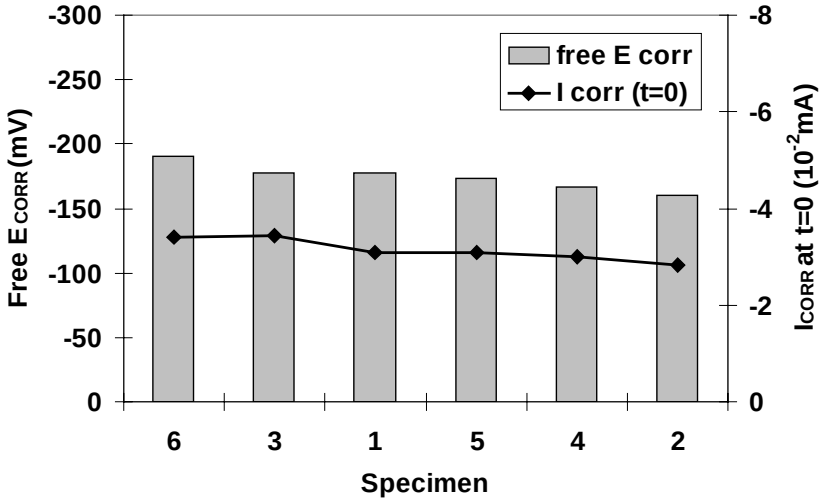

Figure B1: Initial Corrosion Current and Free Corrosion Potential (Series PL-A – 0.40 w/c, plain grout)

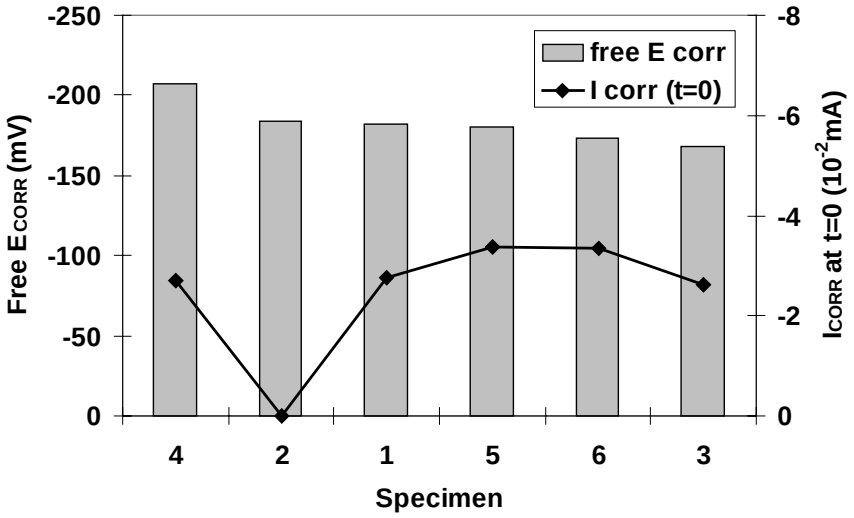

Figure B2: Initial Corrosion Current and Free Corrosion Potential (Series AB-A1 – 0.33 w/c, 2% anti-bleed, strand A)

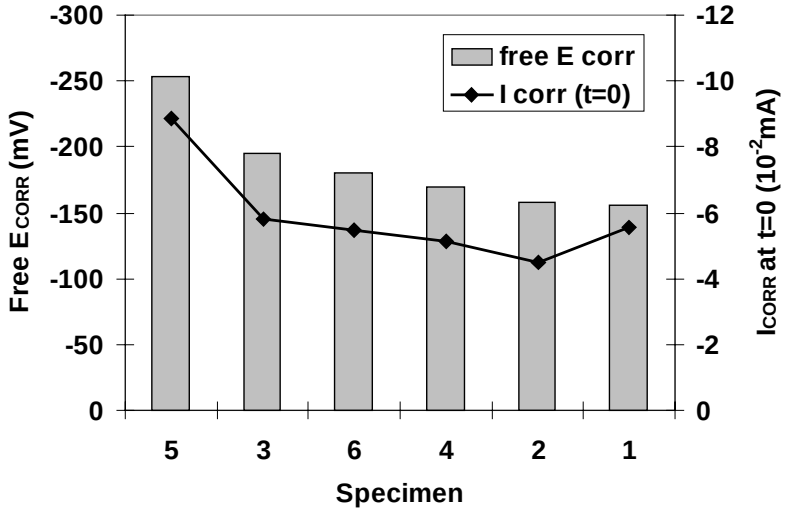

Figure B3: Initial Corrosion Current and Free Corrosion Potential (Series FA-A – 0.35 w/c, 30% fly ash, 4 ml/kg superplasticizer, strand B)

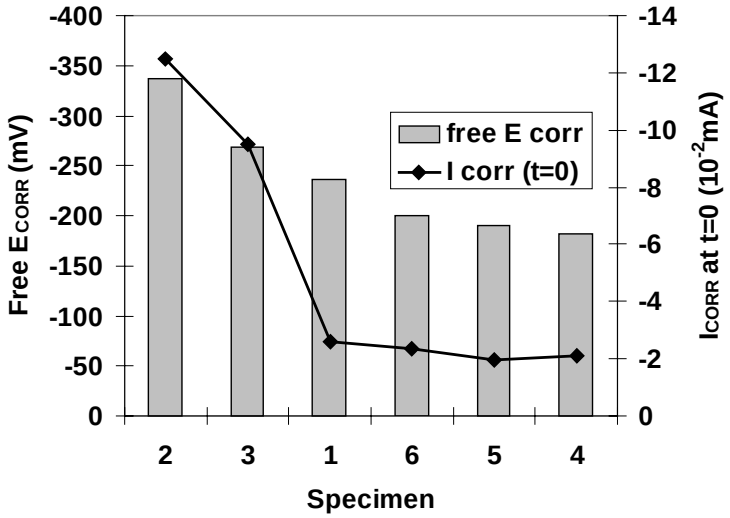

Figure B4: Initial Corrosion Current and Free Corrosion Potential (Series SF-A – 0.35 w/c, 15% silica fume, 16 ml/kg superplasticizer, Strand A)

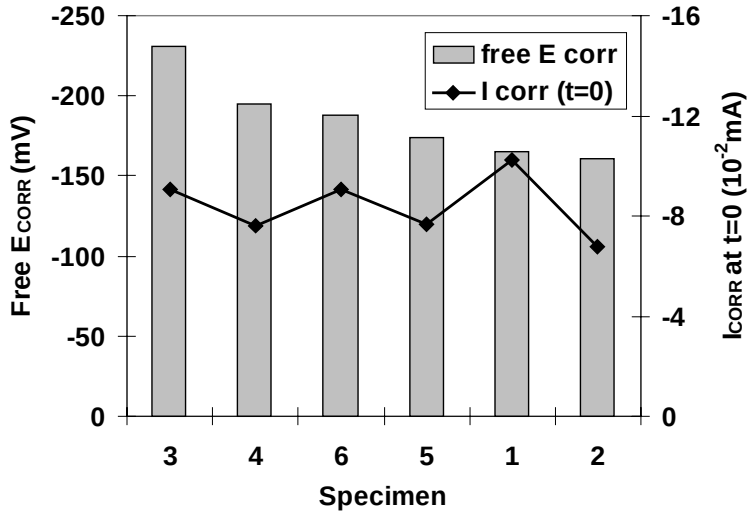

Figure B5: Initial Corrosion Current and Free Corrosion Potential (Series AB-B – 0.33 w/c, 2% anti-bleed, Strand B)

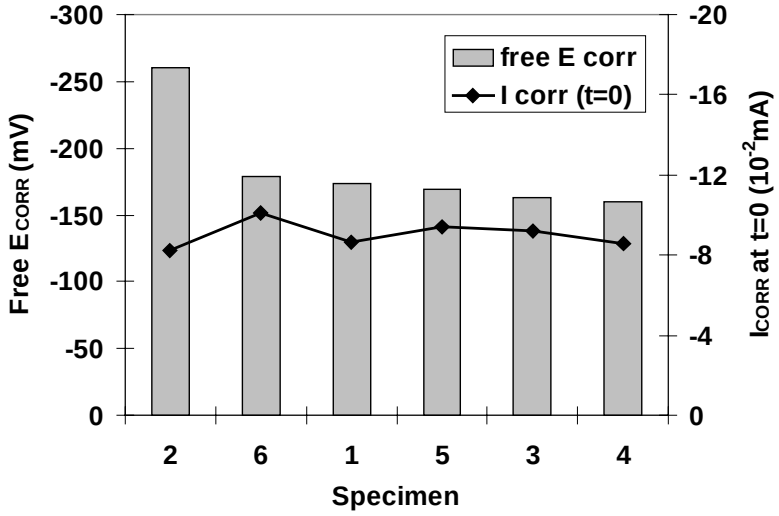

Figure B6: Initial Corrosion Current and Free Corrosion Potential (Series AB-A2 – 0.33 w/c, 2% anti-bleed, Strand A)

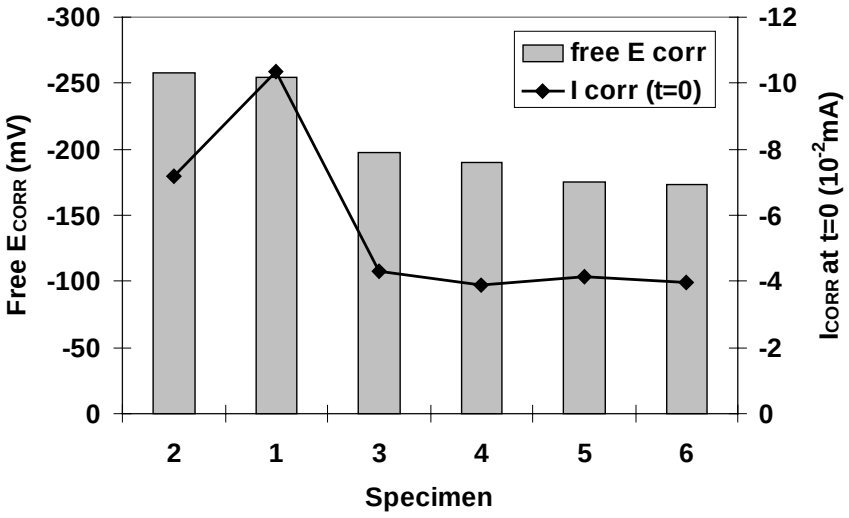

Figure B7: Initial Corrosion Current and Free Corrosion Potential (Series FA-B – 0.35 w/c, 30% fly ash, 4 ml/kg superplasticizer, Strand B)

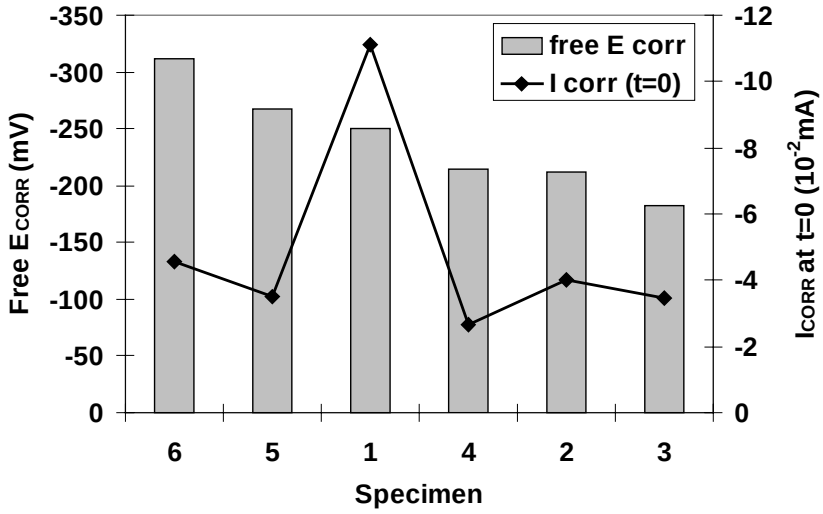

Figure B8: Initial Corrosion Current and Free Corrosion Potential
(Series SF-B – 0.35 w/c, 15% silica fume, 16 ml/kg superplasticizer, Strand B)

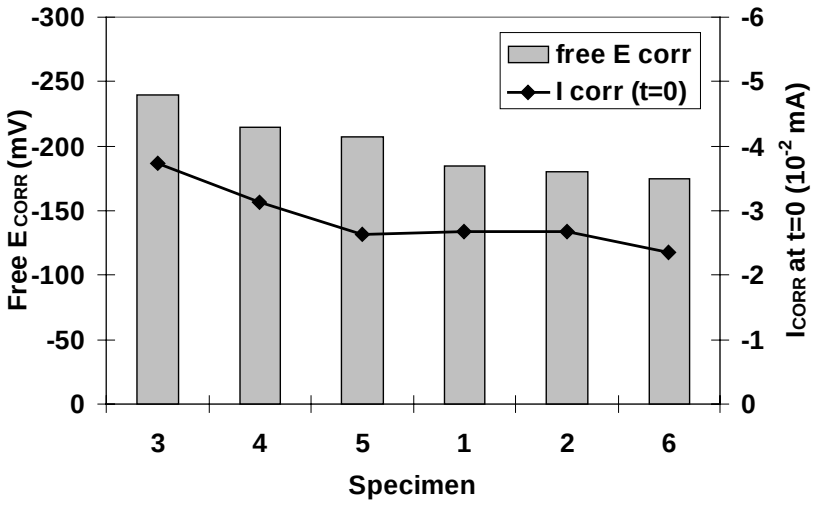

Figure B9: Initial Corrosion Current and Free Corrosion Potential
(Series TX-A – 0.44 w/c, 0.9% expansive admixture)

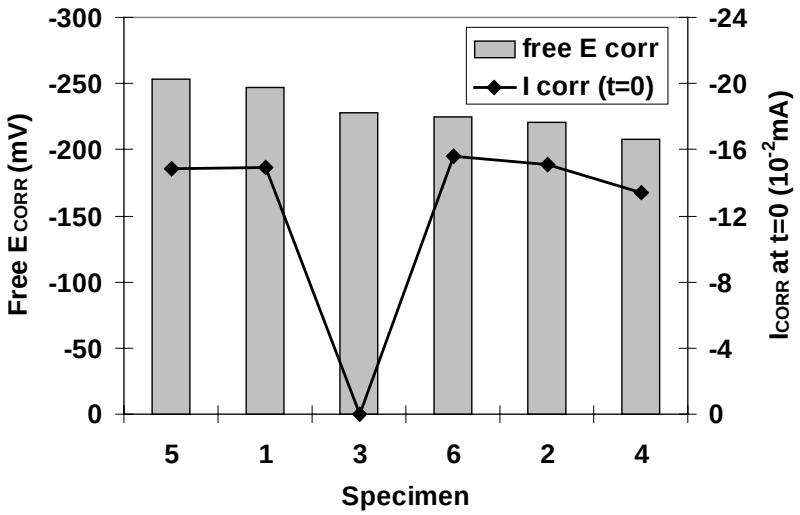

Figure B10: Initial Corrosion Current and Free Corrosion Potential (Series TX-B – 0.44 w/c, 0.9% expansive admixture)

APPENDIX C

TIME TO CORROSION VERSUS FREE CORROSION POTENTIAL

Figures C1-C10 give a comparison of the time to corrosion (T_{corr}) and the free corrosion potential (free E_{corr}) for each of the grouts tested in the accelerated corrosion testing phase. There appears to be little correlation between the free corrosion potential and the time to corrosion for the grouts within a series.

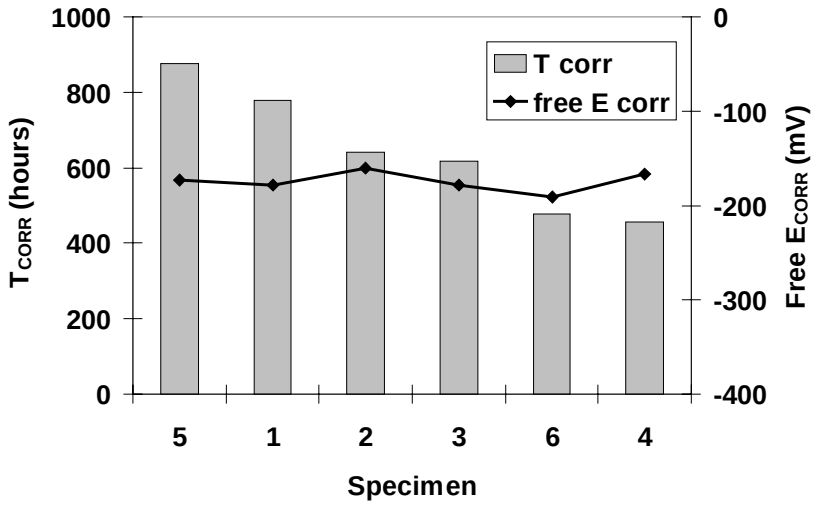

Figure C1: Average Time to Corrosion and Free Corrosion Potential (Series PL-A – 0.40 w/c, plain grout)

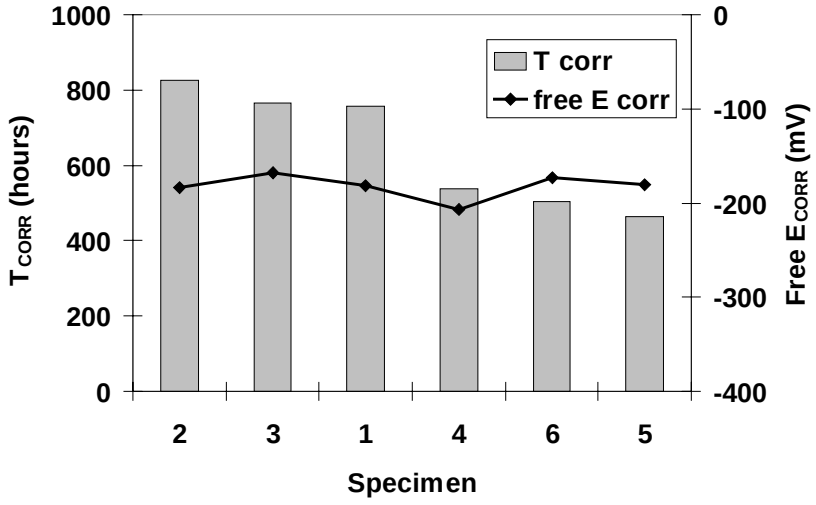

Figure C2: Average Time to Corrosion and Free Corrosion Potential (Series AB-A1 – 0.33 w/c, 2% anti-bleed, strand A)

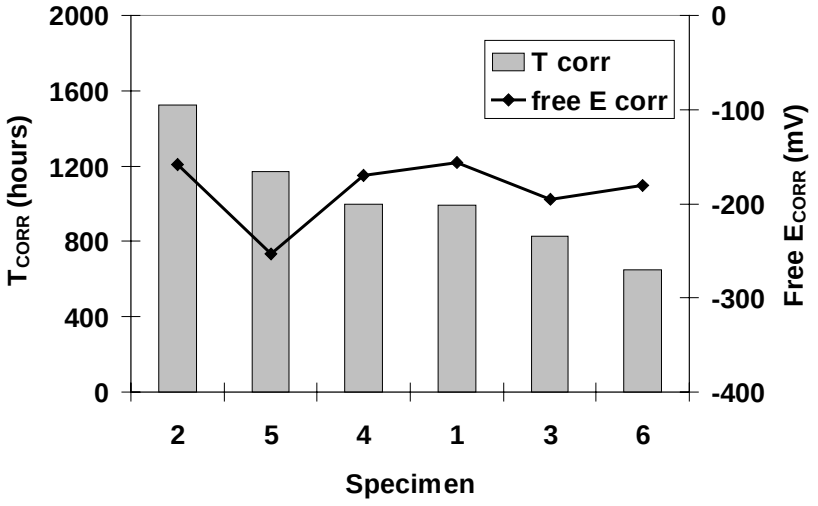

Figure C3: Average Time to Corrosion and Free Corrosion Potential (Series FA-A – 0.35 w/c, 30% fly ash, 4 ml/kg superplasticizer, strand B)

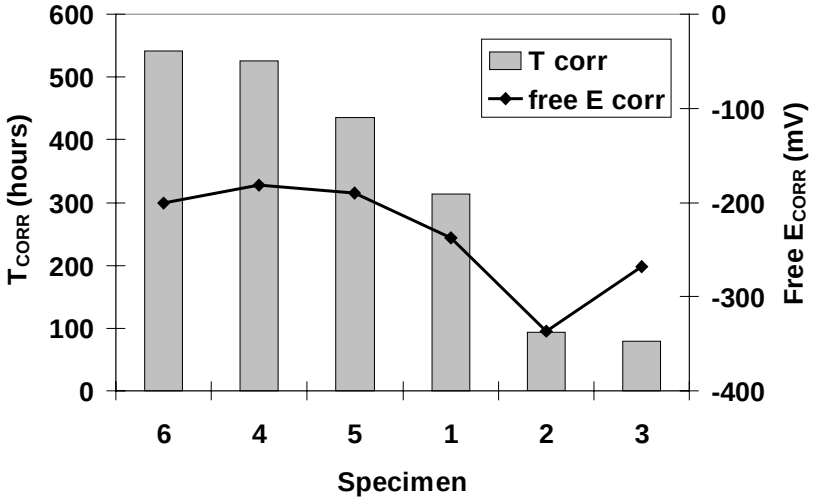

Figure C4: Average Time to Corrosion and Free Corrosion Potential (Series SF-A – 0.35 w/c, 15% silica fume, 16 ml/kg superplasticizer, Strand A)

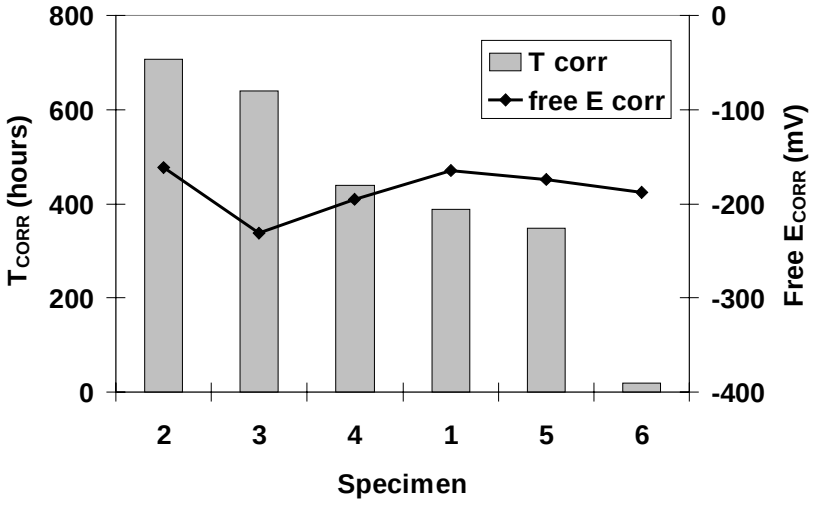

Figure C5: Average Time to Corrosion and Free Corrosion Potential (Series AB-B – 0.33 w/c, 2% anti-bleed, Strand B)

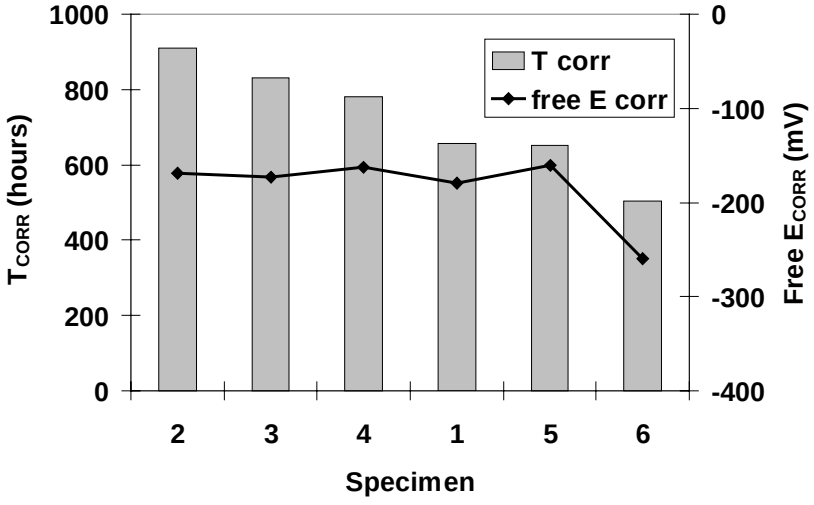

Figure C6: Average Time to Corrosion and Free Corrosion Potential (Series AB-A2 – 0.33 w/c, 2% anti-bleed, Strand A)

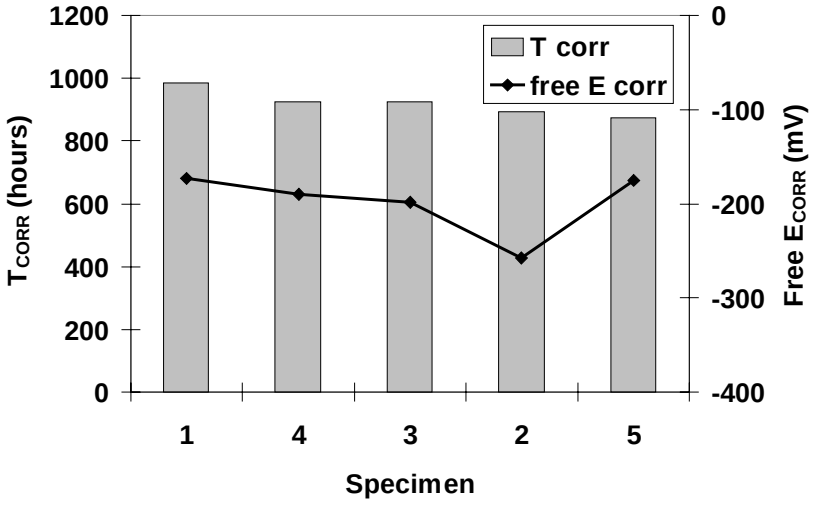

Figure C7: Average Time to Corrosion and Free Corrosion Potential (Series FA-B – 0.35 w/c, 30% fly ash, 4 ml/kg superplasticizer, Strand B)

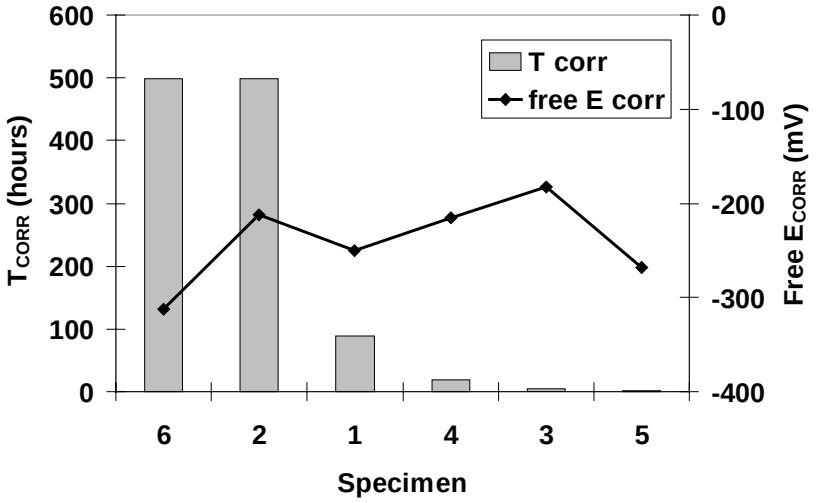

Figure C8: Average Time to Corrosion and Free Corrosion Potential (Series SF-B – 0.35 w/c, 15% silica fume, 16 ml/kg superplasticizer, Strand B)

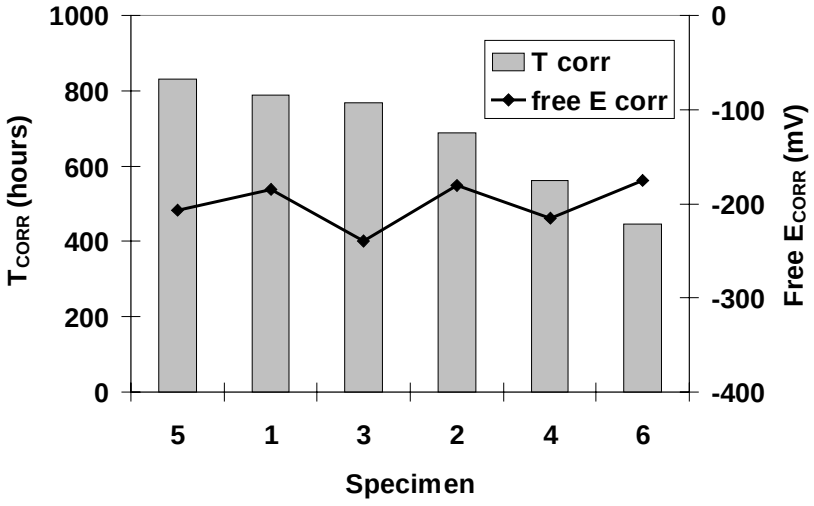

Figure C9: Average Time to Corrosion and Free Corrosion Potential (Series TX-A – 0.44 w/c, 0.9% expansive admixture)

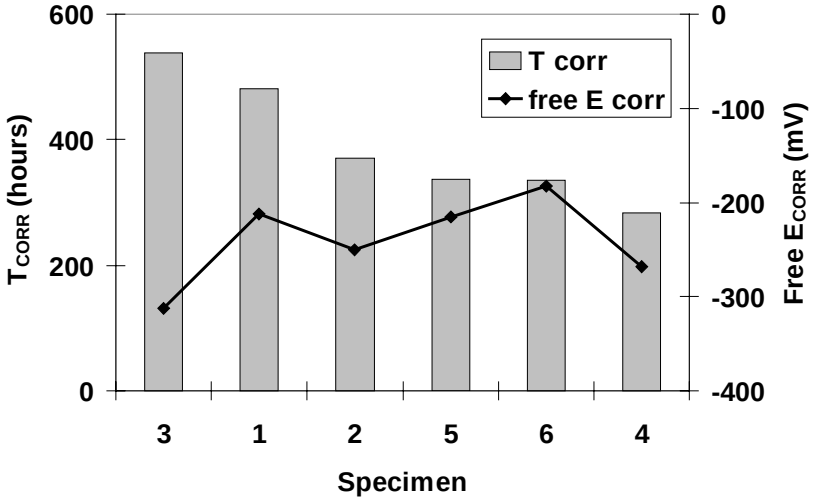

Figure C10: Average Time to Corrosion and Free Corrosion Potential (Series TX-B – 0.44 w/c, 0.9% expansive admixture)

BIBLIOGRAPHY

1. **Aitcin, P., Ballivy, G. and Parizeau, R.,** "The Use of Condensed Silica Fume in Grouts," *Innovative Cement Grouting,* SP-83, American Concrete Institute, 1984, pp. 1-18.

2. **American Society for Testing and Materials,** *Standard Test Method for Compressive Strength of Grouts for Preplaced Aggregate Concrete in the Laboratory*, ASTM C942-86, Philadelphia, PA, 1986.

3. **American Society for Testing and Materials,** *Standard Test Method for Expansion and Bleeding of Freshly Mixed Grouts for Preplaced-Aggregate Concrete in the Laboratory*, ASTM C940-87, Philadelphia, PA, 1987.

4. **American Society for Testing and Materials,** *Standard Test Method for Flow of Grout for Preplaced-Aggregate Concrete (Flow Cone Method)*, ASTM C939-94a, Philadelphia, PA, 1994.

5. **American Society for Testing and Materials,** *Standard Test Method for Time of Setting of Grouts for Preplaced-Aggregate Concrete in the Laboratory*, ASTM C9533-87, Philadelphia, PA, 1987.

6. **Berke, N.S.,** "Corrosion Inhibitors in Concrete," *Concrete International,* July 1991, pp. 24-27.

7. **Berke, N.S. et al.,** "Protection Against Chloride-Induced Corrosion," *Concrete International: Design and Construction*, Vol. 10, No. 12, December 1998, pp. 45-55.

8. **Berke, N.S.,** "Resistance of Microsilica Concrete to Steel Corrosion, Erosion and Chemical Attack," *Fly Ash, Silica Fume, Slag, and Natural Pozzolans in Concrete: Proceedings of the Third International Conference,* Trondheim, Norway, SP-114, V.M. Malhotra, Ed., 1989, pp. 861-886.

9. **Berke, N.S., Shen, D.F. and Sundberg, K.M.,** "Comparison of Current Interruption and Electrochemical Impedance Techniques in the Determination of Corrosion Rates of Steel in Concrete," *The Measurement and Correction of Electrolyte Resistance in Electrochemical Tests, STP 1056,* L.L. Scribner and S.R. Taylor, Eds, American Society for Testing and Materials, Philadelphia, PA, 1990, pp. 191-201.

10. **Diederichs, U. and Schutt, K.,** "Silica Fume Modified Grouts for Corrosion Protection of Post-Tensioning Tendons," *Fly Ash, Silica Fume, Slag, and Natural Pozzolans in Concrete: Proceedings of the Third International Conference,* Trondheim, Norway, SP-114, V.M. Malhotra, Ed., 1996, pp. 1173-1195.

11. **Domone, P.L. and Jefferis, S.A.,** *Structural Grouts,* Blackie Academic & Professional, London, 1994.

12. **Domone, P.L. and Tank, S.B.,** "Use of Condensed Silica Fume in Portland Cement Grouts," *Fly Ash, silica Fume, Slag, and Natural Pozzolans in Concrete: Proceedings, Second International Conference,* Madrid, Spain, SP 91-61, V.M. Malhotra, Ed., 1986, pp. 1232-1260.

13. **Ehrhardt, W.C.,** "IR Drop in Electrochemical Corrosion Studies – Part I: Basic Concepts and Estimates of Possible Measurement Errors," *The Measurement and Correction of Electrolyte Resistance in Electrochemical Tests, STP 1056,* L.L. Scribner and S.R. Taylor, Eds., American Society for Testing and Materials, Philadelphia, PA, 1990, pp. 27-58.

14. **Fidjestol, P.,** "Reinforcement Corrosion and the Use of CSF-Based Additives," *Concrete Durability: Katherine and Bryant Mather International Conference,* SP-100, J.M. Scanlon, Ed., 1987, pp. 1445-1458.

15. **Hamilton, H.R., III,** "Investigation of Corrosion Protection Systems for Bridge Stay Cables," *Ph.D. Dissertation,* The University of Texas at Austin, September 1995.

16. **Hope, B.B. and Ip, A.K.,** "Corrosion Inhibitors for Use in Concrete," *ACI Materials Journal,* November-December 1989, pp. 602-608.

17. **Koester, B.D.,** "Evaluation of Cement Grouts for Strand Protection Using Accelerated Corrosion Tests," *Masters Thesis,* The University of Texas at Austin, December 1995.

18. **Lankard, D.R., Thompson, N., Sprinkel, M.M. and Virmani, Y.P.,** "Grouts for Bonded Post-Tensioned Concrete Construction: Protecting Prestressing Steel from Corrosion," *ACI Materials Journal,* September-October 1993, pp. 406-414.

19. **Montani, R.,** "Concrete Repair and Protection with Corrosion Inhibitor*," Proceedings of the Seventh International Conference on Structural Faults and Repair,* Volume 2, Edinburgh, Scotland, 1997, pp. 253-264.

20. **Mott MacDonald,** *Sika Ferrogard® 901 & 903 Corrosion Inhibitors: Evaluation of Test Programme,* August 1996.

21. **Nmai, C.K.,** "Corrosion-Inhibiting Admixtures: Passive, Passive-Active versus Active Systems," *Advances in Concrete Technology: Proceedings of the Second CANMET/ACI International Symposium,* Las Vegas, Nevada, SP-154, V.M. Malhotra, Ed., 1995, pp. 565-585.

22. **Perenchio, W.F., Fraczek, J. and Pfeifer, D.W.,** "Corrosion Protection of Prestressing Systems in Concrete Bridges," NCHRP Report 313, Transportation Research Board, Washington, D.C., February 1989.

23. **Post-Tensioning Institute,** "Guide Specification for Grouting of Post-Tensioned Structures," *PTI Committee on Grouting Specifications, 5th Draft,* November 1997.

24. **Ranish, E.H., Rostasy, F.S. and Herschelmann, F.,** "Properties of Cement Grouts with Silica Fume Addition for the Injection of Post-Tensioning Ducts," *Fly Ash, Silica Fume, Slag, and Natural Pozzolans in Concrete: Proceedings of the Third International Conference,* Trondheim, Norway, SP-114, V.M. Malhotra, Ed., 1996, pp. 1159-1171.

25. **Schokker, A.J.,** "Improving Corrosion Resistance of Post-Tensioned Substructures Emphasizing High Performance Grouts," *Ph.D. Dissertation,* The University of Texas at Austin, May 1999.

26. **Schupack, M.,** "Admixture for Controlling Bleed in Cement Grout Used in Post-Tensioning," *Journal of the Prestressed Concrete Institute,* November-December 1974.

27. **Schupack, M.,** "Grouting Tests on Large Post-Tensioning Tendons for Secondary Nuclear Containment Structures," *Journal of the Prestressed Concrete Institute,* March-April 1971, pp. 85-97.

28. **Schupack, M. and Suarez, M.G.,** "Some Recent Corrosion Embrittlement Failures of Prestressing Systems in the United States," *Journal of the Prestesssed Concrete Institute,* March-April 1982.

29. **Shaw, M.,** "Migrating Corrosion Inhibitors for Reinforced Concrete Protection*," Proceedings of the Seventh International Conference on Structural Faults and Repair,* Volume 2, Edinburgh, Scotland, 1997, pp. 317-324.

30. **Sprinkel, M.,** "High Performance Silica Fume Grout for Post-Tensioning Ducts," *Proceedings of the PCI/FHWA International Symposium on High Performance Concrete,* L.S. Johal, ed., New Orleans, LA, 1997, pp. 343-354.

31. **Swamy, R.N.,** "Design for Durability and Strength Through the Use of Fly Ash and Slag in Concrete," *Advances in Concrete Technology: Proceedings of the Third CANMET/ACI International Conference,* Auckland, New Zealand, SP-171, V.M. Malhotra, Ed., 1997, pp. 1-71.

32. **Thompson, N.G., Lankard, D. and Sprinkel, M.,** "Improved Grouts for Bonded Tendons in Post-Tensioned Bridge Structures," *Report No. FHWA-RD-91-092, Federal Highway Administration,* Cortest Columbus Technologies, January 1992.

33. **West, J.S.,** "Durability Design of Post-Tensioned Bridge Substructures," *Ph.D. Dissertation,* The University of Texas at Austin, May 1999.

34. **Whiting, D. and Detwiler, R.,** "Silica Fume Concrete for Bridge Decks," *NCHRP Report 410, National Cooperative Highway Research Program,* National Academy Press, Washington, D.C., 1998.

35. **Working Party of the Concrete Society, "**Durable Bonded Post-Tensioned Concrete Bridges," Technical Report No. 47, August 1996.